FINAL REPORT

FURTHER STUDIES OF A TRUSSED-WEB GIRDER COMPOSED OF REINFORCED PLASTICS

by

Fred C. McCormick
Faculty Research Engineer
Virginia Highway & Transportation Research Council
and
Professor of Civil Engineering
University of Virginia

and

Husamettin Alper
Graduate Research Assistant

Virginia Highway & Transportation Research Council
(A Cooperative Organization Sponsored Jointly by the Virginia Department of Highways & Transportation and the University of Virginia)

Charlottesville, Virginia

November 1975
VHTRC 76-R16

SUMMARY

Three single section and one trisection girders eight feet long were fabricated and load tested to determine the deflection, strain, and creep characteristics of the members. One specimen fabricated with stranded elements composed of Kevlar 49 instead of glass exhibited improved stiffness properties. The maximum load applied to a specimen was 600 psf uniformly distributed over the top plate, which caused failure of the top stiffener joints. A ratio of 107 for live load to dead weight was obtained in this test. Partial loading of the girder caused elastic buckling of some web elements. Analytical studies showed that buckling could be prevented by the addition of dead weight as a concrete slab on the top plate. A center span deflection creep test at a load of 150 psf indicated a secondary creep rate of 0.03 inch/year, with a termination of primary creep after 30 days.

The test specimens just met the center span deflection requirements of AASHTO for an 85 psf live load.

Computations for strains and deflections based on elastic strain-energy theories were 20% and 30% higher than experimental values for deflections and strains, respectively. Partial loading tests verified the application of the principle of superposition in the analytical procedures.

It is recommended that a field study of a prototype pedestrian bridge be conducted to extend the findings of the laboratory studies.

TABLE OF CONTENTS

TABLE OF CONTENTS (cont.)

FINAL REPORT

FURTHER STUDIES OF A TRUSSED-WEB GIRDER COMPOSED OF REINFORCED PLASTICS

by

Fred C. McCormick
Faculty Research Engineer
Virginia Highway & Transportation Research Council
and
Professor of Civil Engineering
University of Virginia

and

Husamettin Alper
Graduate Research Assistant

INTRODUCTION

The investigations conducted in this project were extensions and modifications of studies completed in June 1974 and described in a final report by McCormick.[1] The earlier study indicated the relationship between a theoretical stress analysis and experimental test results and provided performance characteristics for laboratory specimens when load tested. In addition, the previous work provided insight for fabrication procedures and utilization of reinforced plastics for primary structural components.

The current project extended from June 1, 1974 to October 1, 1975. All experimental and analytical work was focused upon the same geometric configuration used in the previous studies. Figure 1 shows the principal features of a typical test specimen. A detailed description of modifications to the member is included in a subsequent section. The major effort was directed toward the fabrication, testing, and analysis of a multisection test specimen composed of three similar units joined at their top flanges by a glass reinforced plastic (GRP) cover plate. Other single specimen investigations included creep and fatigue tests.

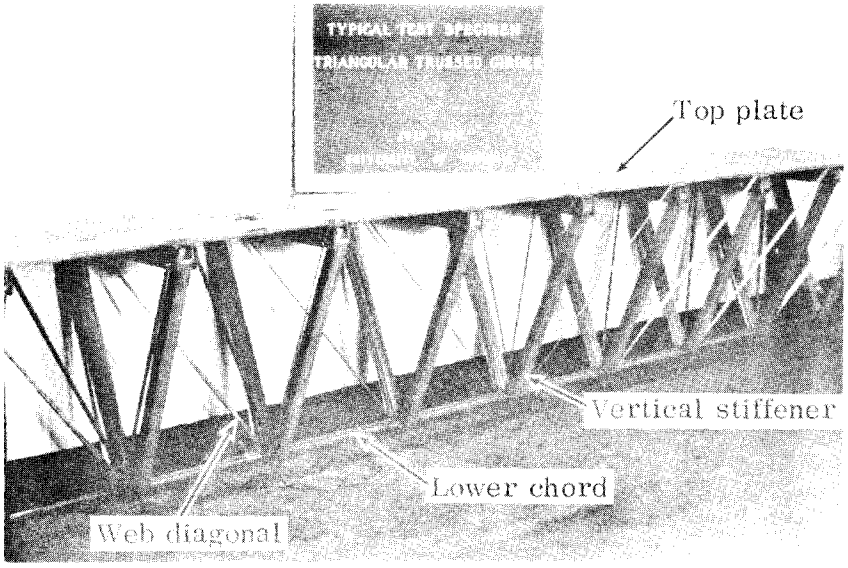

Figure 1. Typical test specimen of a single unit, triangular trussed girder.

OBJECTIVES

The specific work objectives are listed below in two categories: those growing out of previous work and those involving expanded investigations.

A. Continuing Investigations

1. Revise the top plate assembly to improve the strength development of the flexural member.

2. Study the flexural creep behavior of typical test specimens.

3. Study the geometric configurations of the member in an effort to optimize the dimensional relationships of the triangular trussed girder (TTG) arrangement.

B. Expanded Investigations

1. Survey the fatigue characteristics of reinforced resin materials systems in typical highway service conditions.

2. Fabricate, test, and analyze a multisection TTG specimen with modifications from previous design concepts as suggested by the findings from the previous investigation and the program outlined in A above.

3. Expand contacts and discussions with manufacturing representatives relative to production costs and fabrication techniques.

4. Provide recommendations for the feasibility of a modest field installation and study of an experimental bridge composed of reinforced plastics.

The achievement of these objectives is described along with pertinent findings and recommendations in the sections which follow.

MODIFICATIONS IN JOINTS AND ELEMENTS

Revisions to Top Plate and Stiffener Connections

The successful performance of the top plate connection for the triangular trussed girder (TTG) specimen number 5 (see Figure 2) was reported previously. However, it was recognized that several inefficiencies existed in this connection due to the sequential assembly steps required for complete fabrication. Therefore, as a first effort in this study, the top plate connection at each panel point was modified as shown in Figure 3. The addition of one bolt through the top plate and transverse stiffener tube eliminated the wraparound strands of roving which attached the plate and channel. Also, the use of a small steel pin at the joint between the web stiffener and the transverse tube eliminated another group of glass strands connecting these elements. The sizes of the steel bolts and pins shown were used for convenience only. A noncorrosive metal or nonmetallic material could be used for these mechanical connectors equally as well. Prior to installation of the bolt, the top plate was bonded to the transverse tube with polyester resin. No resin was used in the connection for the tubes.

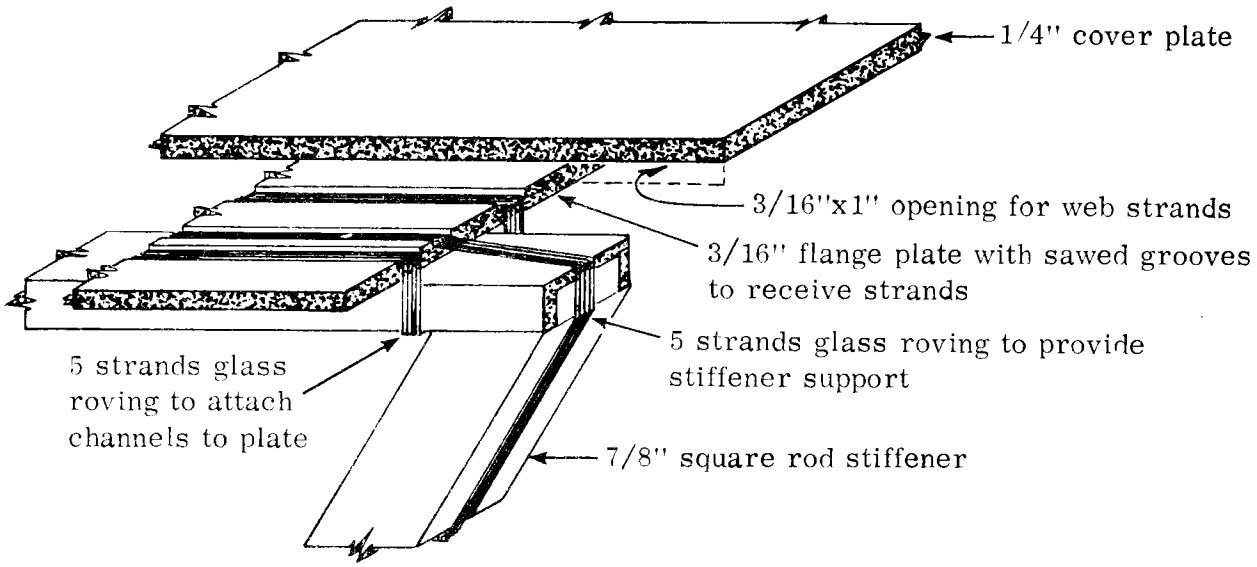

Figure 2. Top-flange assembly details of specimen TTG-5.

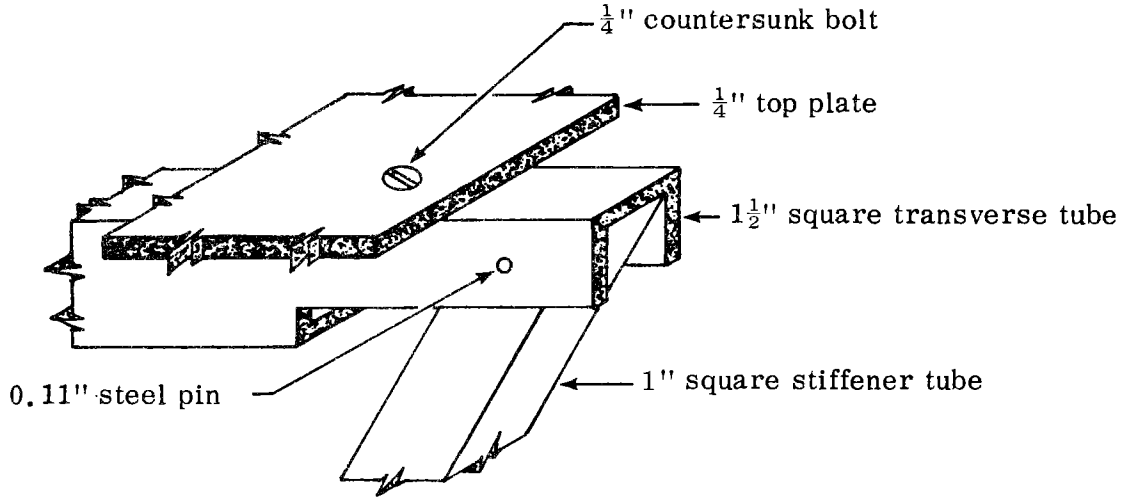

Figure 3. Modified connection at top plate of TTG-7.

Revisions to Stiffening Elements

Both the top plate and web stiffeners were changed in the fabrication of TTG-7 from those used in previous specimens. Figure 2 shows the original design used for TTG-5 and Figure 3 shows details of TTG-7. Glass reinforced tubes with 1/8-inch wall thickness were for the stiffeners in TTG-7 with some decrease in the cross sectional area. In addition, the necessity for precision machining of mating parts was eliminated with the use of the supplementary mechanical fasteners.

Attachment of Stiffeners to Lower Chord

A tee-shaped insert was designed and fabricated to attach the two web stiffeners together at the lower panel point. The insert also provided a bridge between the two stiffeners on which the strands of the lower chord were built up (see Figure 4a). The shape of the insert detailed in Figure 4b was obtained by casting polyester resin in an aluminum mold which had been loosely packed with glass mat to provide reinforcement. Suitable lengths were cut to slip into the open ends of the stiffener tubes.

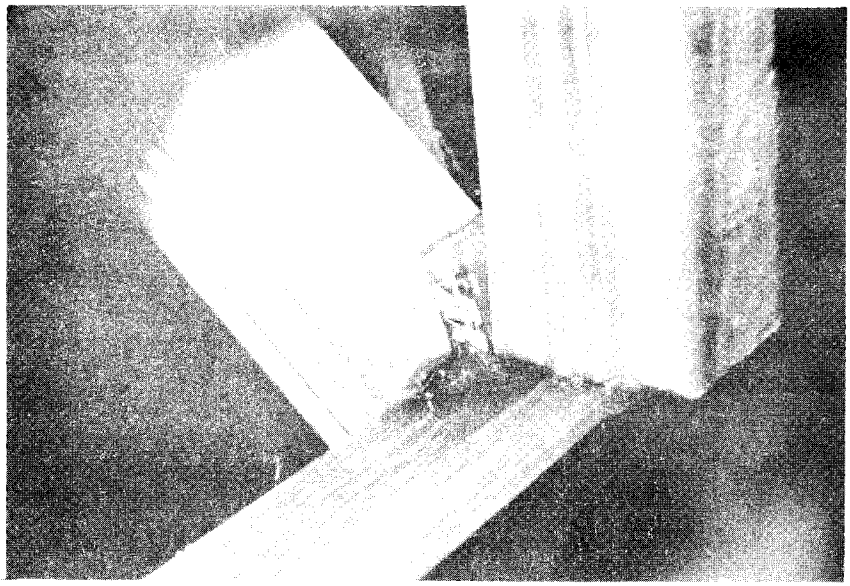

(a) Insert and portion of lower chord and stiffener.

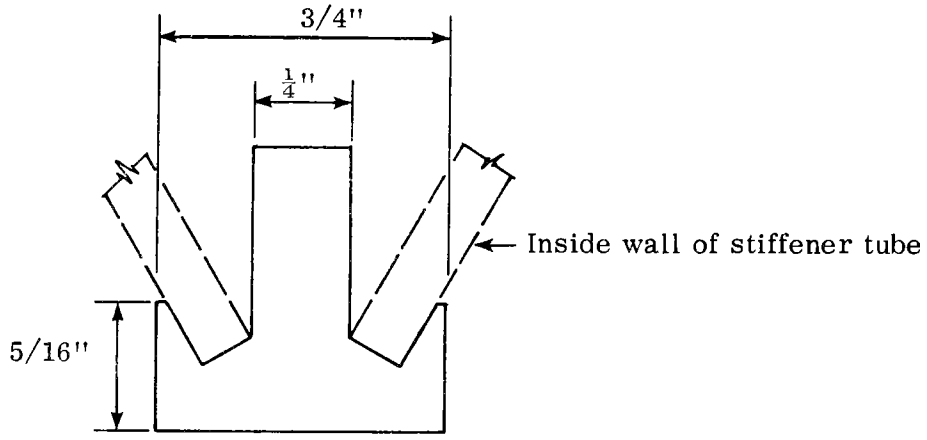

(b) Details of cross section

Figure 4. Insert for connecting stiffeners at lower chord positions.

PERFORMANCE OF MODIFIED TEST SPECIMENS

Fabrication

Specimen TTG-7 was fabricated with the modifications described in the preceeding section and with width and depth dimensions of 16 and 17 inches, respectively. The weight of this member was 36.1 pounds. The addition of a bonded cover plate 1/4-inch thick increased the weight to 59.5 pounds. In the fabrication of the girder, the transverse plate stiffeners were attached to the top plate and the assembly then was mounted on an eight-foot long plywood mandrel by means of screws. Vertical stiffeners were attached to the plate stiffeners as shown in Figure 3 and also anchored to the mandrel with a single screw. The lower chord inserts were then installed as shown in Figure 4a and manual winding of the lower chord and web elements was completed in approximately two hours. (See Figure 5.) The total assembly and winding time for TTG-7 was approximately the same as that for TTG-5 and 6. However, the modification made for TTG-7 permitted better scheduling of the assembly steps and eliminated one preliminary winding step. It was therefore considered to be an improvement over the procedures used previously. In addition, the use of tubular vertical stiffeners with larger dimensions improved the space requirements for strands during the winding operation. Following a resin curing period of several days at room temperature, eight strain gages were bonded to selected web and chord elements. Subsequently, a 1/4-inch thick GRP cover plate was bonded to the top plate and, finally, a concrete slab 1 1/8-inches thick was cast on the cover plate. Excellent adhesion of the concrete to the cover plate was achieved by means of an expoxy adhesive (Sikadur Hi-Mod, manufactured by SIKA Chemical Corporation, Lyndhurst, New Jersey) applied to the plate just prior to placing the concrete. Other materials used in the fabrication of the girder test specimens were as follows:

1. Glass fiber reinforcing, Type 30, E-glass roving, manufactured by Owens Corning Fiberglass Corporation.

2. Polyester resin 2036 (with MEK peroxide catalyst) with a gel time of about 45 minutes and room temperature cure, manufactured by North American Rockwell Company.

3. Prefabricated plates and shapes of EXTREN 500, manufactured by Morrison Molded Fiber Glass Company.

Specimen TTG-9 was fabricated exactly as TTG-7 with the exception that an organic synthetic fiber, Kevlar 49, manufactured by the E. I. DuPont Company was used in place of glass roving for

the web and lower chord elements. The cross sectional areas of both members are the same. The strand area-to-density ratio of glass-to-Kevlar 49 was 1.06, so the weight of TTG-9 without the cover plate was 36.0 pounds. The tensile modulus of elasticity of Kevlar 49 is approximately twice that of the glass, so an improvement was anticipated in the overall stiffness characteristics of the member.

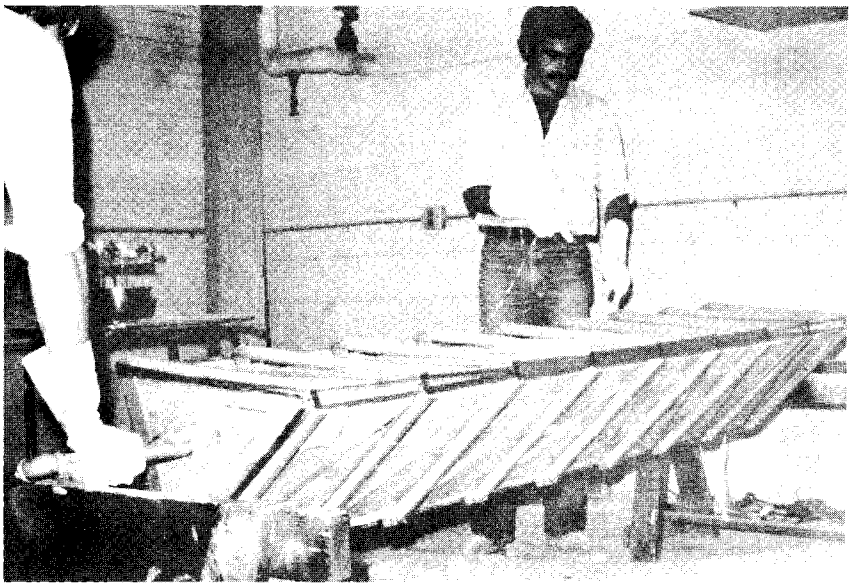

Figure 5. Winding impregnated glass roving to form lower chord and web diagonals of TTG-7. Plywood mandrel was rotated manually.

Load Tests

A series of uniformly distributed loads were applied through an air bag to the top plate of the members to observe the strain and deflection behavior of the specimens. Details of the instrumentation and loading equipment are described in Appendix A. Static loads applied to TTG-7 were as follows:

1. As fabricated to 225 psf
2. With unbonded cover plate to 263 psf
3. With bonded cover plate to 600 psf
4. With bonded concrete slab to 263 psf

Following the static load sequence, cyclic loads were applied to the specimen with the bonded concrete slab for a total of 407,000 cycles. The magnitudes of cyclic loads varied some due to the performance of the loading equipment, but in general, they ranged from a minimum of 108 to a maximum of 188 psf. The load rate ranged from 11 to 15 cycles per minute. It was intended to vary the load from the design value of 100 psf to twice that value, but the performance of the equipment prevented this.

Specimen TTG-9 was loaded to 225 psf with a uniformly distributed load without damage. No further tests were conducted with this member.

Failure Modes

The ultimate strength of TTG-7 was reached at a static load of 600 psf, when the steel pins connecting the stiffeners at the top plate joint began to bend. This resulted in a ratio of approximately 107 for live to dead load. No other damage was observed in any parts of the member, so the actual ultimate strength of the GRP elements was not determined. The pins were replaced with others of the same size and the member reloaded to 360 psf to see if internal damage had occurred in other joints. None was evident from a comparison of load deflection data with those obtained from the specimen during the first load cycle. A second failure of the member occurred after 407,000 applications of cyclic loads described above, when the adhesive joint between the top and cover plates debonded. Inspection of the joint upon removal of the cover plate revealed a relatively large area which had not bonded initially due to an irregularity of the surfaces which prevented good contact when the joint was formed. Apparently a crack propogated through the joint from this region to cause ultimate failure.

Specimen TTG-9 was not loaded to a failure point.

Experimental Deflection Measurements

Vertical deflections due to static loads were measured with mechanical dial indicators located at five lower panel points. The data for the deflection of the center panel point are shown in Figure 6 for some of the load conditions for TTG-7 and TTG-9. A similar deflection curve is shown for TTG-5 for comparison with the performance of the members before structural modifications were made. The slopes of the curves indicate slight progressive improvement in the overall girder deflection as the top flange was stiffened by the use of a cover plate, the concrete slab, and

Kevlar 49 for tension elements. The linearity of the load-deflection relationship shown by the plotted data is typical of the behavior of the member. The linear deformation property was also retained by the member after many cycles of repeated loads. Definitive observations were not made of the complete load-deflection hystersis effects (as an oversight), but it was observed that the dial indicators usually did not return to a zero reading immediately upon the removal of the load. After a period of relaxation (up to 24 hours) however, the residual deflections appeared to disappear. The steeper slope of the curve for specimen TTG-5 (see Figure 2) indicates that the modifications made to TTG-7 degraded the stiffness characteristics of the overall member. Data from deflection indicators located at other panel points confirmed a proportionately greater deflection throughout TTG-7 than in TTG-5. A specific reason for the relative behaviors of the two specimens cannot be offered at this time. It is presumed, however, that the introduction of a truly pinned joint for the connection of the transverse and vertical stiffeners in TTG-7 permitted more in-plane distortion of the three-stiffener assembly than occurred in TTG-5 due to the overwrapped stiffeners and plate. The centerline deflection of TTG-9 was 75% that of TTG-7. This improvement was significant in that the Kevlar 49 constituted only 5.5% by weight of the member. Extensive use of this material, however, must be balanced against a current cost ratio of 20 for Kevlar 49 to E-glass roving.

The limiting centerline deflection for pedestrian bridges as specified by AASHTO[2] is superimposed in Figure 6. Based on the laboratory specimens and test data, specimen TTG-7 with a cover plate and TTG-9 without a cover plate would meet the requirements for an 85 psf live load.

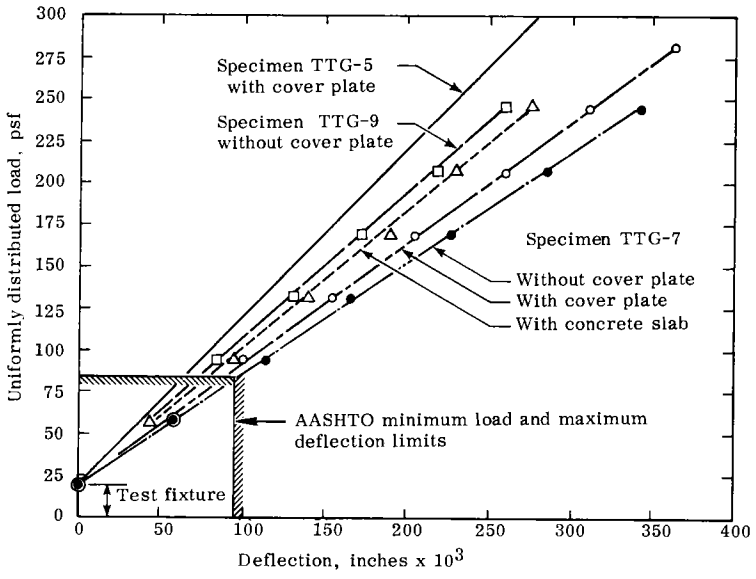

Figure 6. Centerline deflection of girders with uniformly distributed load.

Experimental Strain Measurements

Measurements of unit strains along the axial directions of selected tension elements were made during the series of loads described for the deflection measurements. The measured strains may be transformed directly to unit stresses by multiplying by the tensile modulus of 7×10^6 psi.

Figure 7 presents the load-stress results for specimen TTG-7. The relationship was typically linear as demonstrated by the points plotted for the best fit curves of gages 4, 5, 6 and 8. The data indicated a pronounced change in the slope of the curves at a load of 300 psf. This change was observed with repeated load tests. The cause of this behavior is not known precisely, but it may have been due to a change in the restraint conditions of a joint or at the end support. Theoretically, the strain in gage 8 should be zero, based on small displacement and roller support assumptions. The indicated strain is believed to have resulted from frictional restraint of the end stiffeners in the supports, from reaction forces generated by strands anchored from the adjacent panel, or from a combination of all effects.

Ideally, all of the load-strain curves should be coincident in Figure 7 in order for each element to be stressed equally. The close grouping of the web-element strains (gages 1, 2 and 3) represents an efficient use of the material in these elements and is probably about as effective as will be possible given the design and fabrication procedures used. Neither the grouping nor relative positions of the curves for gages 4, 5 and 6 are considered to be good. A slight modification of the winding sequence of the roving strands should provide considerable improvement in the stress development in the various elements.

Figure 8 shows the effect of the various cover plates upon the strains in the most highly strained element (gage 2) of TTG-7. The performance of the same web elements in specimens TTG-5 and TTG-9 are also compared with these effects. The slopes of the load-strain curves are recorded to provide a quantitative measure of differences in the strain effects. From the five curves shown, the strain was the greatest in TTG-7 with the bonded cover plate and the least in TTG-7 with the concrete slab. Using the differences in slopes as a basis, the tests indicated that there was a strain improvement of 18% with the addition of the concrete slab to TTG-7; 11% with the substitution of Kevlar for glass roving; and 6% with the joint configuration of TTG-5.

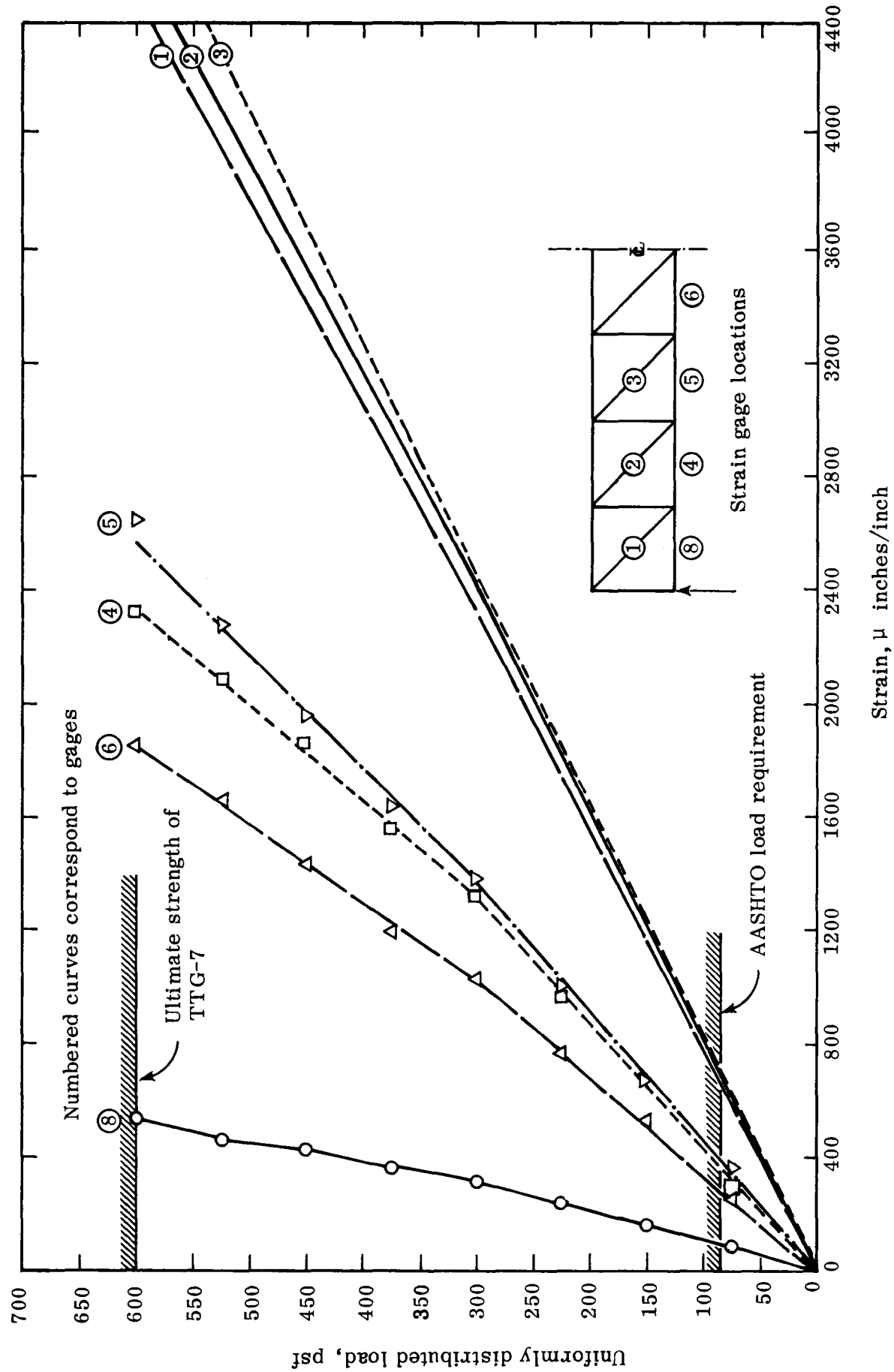

Figure 7. Strain of web and lower elements in load test of TTG-7 with bonded cover plate.

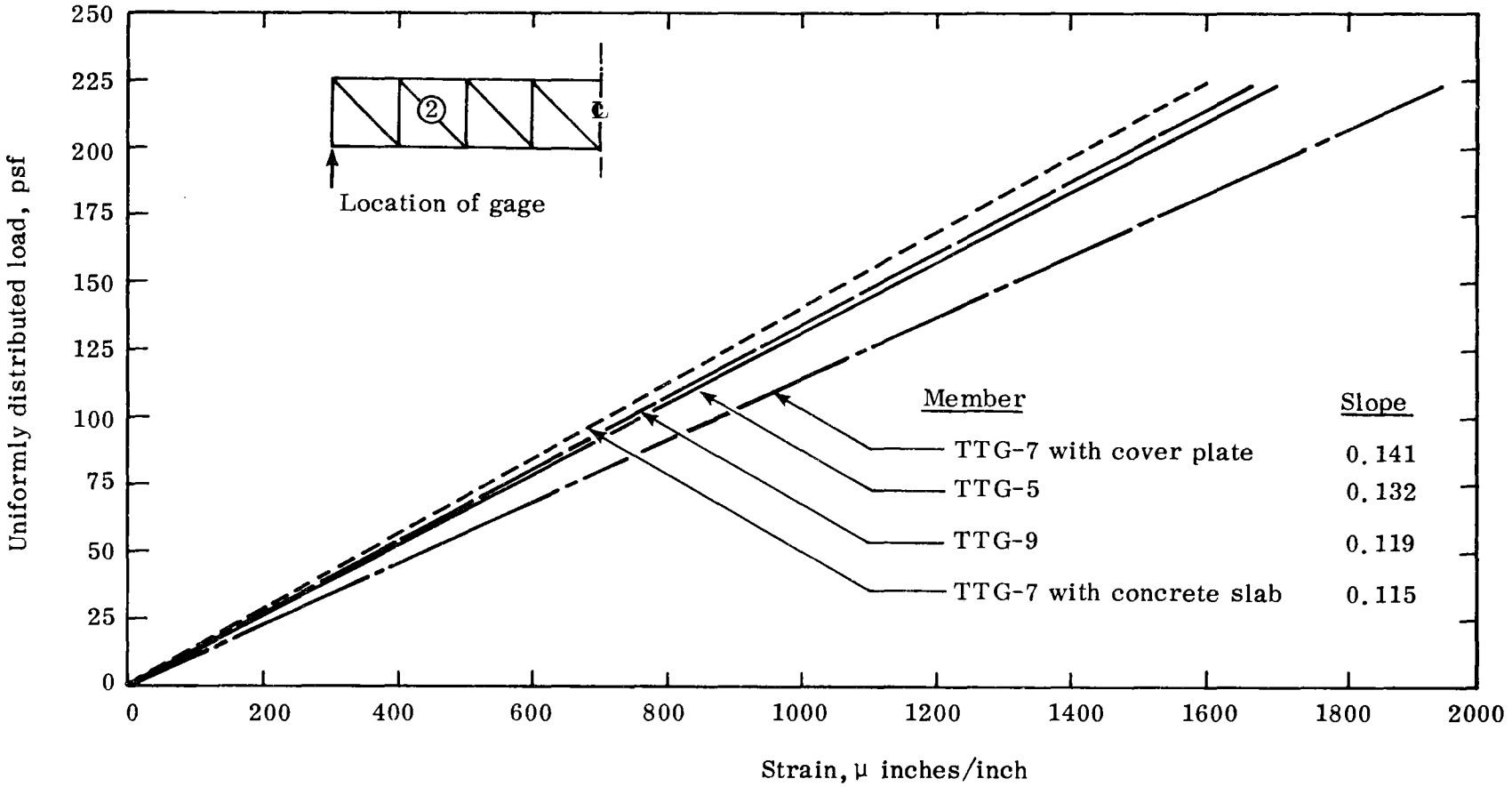

Figure 8. Comparison of strain in a web diagonal for various members with uniform load.

Stress Considerations and Safety Factors

As stated previously, the ultimate strength of TTG-7 was determined by excessive joint deformation due to bending of steel pins connecting the stiffeners. Figure 7 graphically compares the ultimate load of 600 psf with the load requirement of 85 psf by AASHTO. This load ratio provides a safety factor of 7. The calculated stress in the most highly strained element (gage 3) was 4,480 psi at the 85 psf load level. This stress provides a safety factor of 22 based on an assumed ultimate stress of 100,000 psi for the glass strands. The highest calculated stress was 35,000 psi (gage 3) when the load test was terminated. Therefore, no determination of the actual in-place strength of the tension strands was made during the series of static load tests. However, at the conclusion of the cyclic load test of TTG-7, broken fibers were observed where web strands passed over the lower edge of a stiffener. These fibers obviously had been cut by the sharp edge of the stiffener as the member underwent repetitive displacements.

Comparison of Analytical and Experimental Results for TTG-7

Method of Analysis

Computations were made for strains in the truss elements and for displacements at the joints based on linear elastic strain-energy theory. The solution provided for three-dimensional translation of joints, axial strains in the truss elements, and bending of the top plates. Direct application was made of elastic constants determined from laboratory tests for the various materials used. Stiffness matrices were used to adapt the computations for solution by a digital computer. A detailed description of the computational procedure and computer program are included in Appendix A.

Comparison of Deflections

Figure 9 shows a comparison between the analytical and experimental results of the vertical deflections at the centerline of the span of TTG-7 with a bonded cover plate and a concrete slab. The results in Figure 9 are within anticipated performance in view of the unknown stiffness characteristics of the actual joints, some uncertainty in the elastic constants of the materials, and the assumed restraint conditions of the supports during testing. No effort was made to adjust the "fit" relationship of the theoretical solution with the experimental data by use of empirical

constants or other devices. Additional performance experience with this type of structural member may justify future modification of the analysis to account for unknown factors and to provide a better prediction of behavior for design considerations. It should be noted that the predicted deflections for the member with the cover plate only were greater than those measured experimentally. This result would suggest that the joints exhibited some degree of rigidity during the load test in contrast with the assumed pinned conditions.

Comparison of Strains

Figure 10 shows a comparison between the analytical and experimental strains in the most highly strained tension element. Similar comparisons were studied for the other web and lower chord elements. Deviations ranged from 20% to 28% for these elements, which values are larger than those shown in Figure 10. As in the case of the deflections, the curves shown in Figure 10 were unadjusted. Agreement of the strain data was not as close as for the deflection data and perhaps should be considered unacceptable. However, the predicted strain values for all elements were greater than the corresponding measured values, which would result in a somewhat conservative design if used directly for sizing the areas of elements. It should also be noted that the stiffness characteristics (deflections) of the girder would undoubtedly control the size of the elements of the member. Therefore, the development of lower than predicted strains (and proportionately, stresses) would improve the reserve strength of the member and, as long as economic considerations were not exceeded, should enhance the overall performance of the girder.

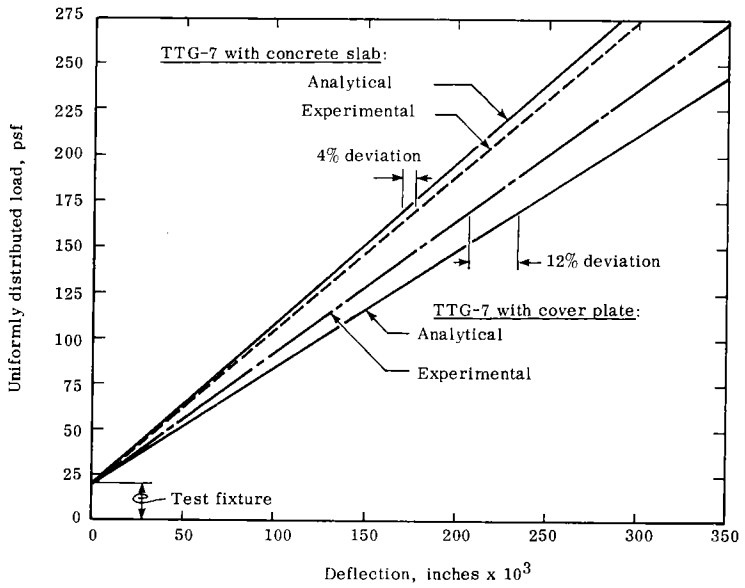

Figure 9. Comparison of analytical and experimental centerline deflections of TTG-7.

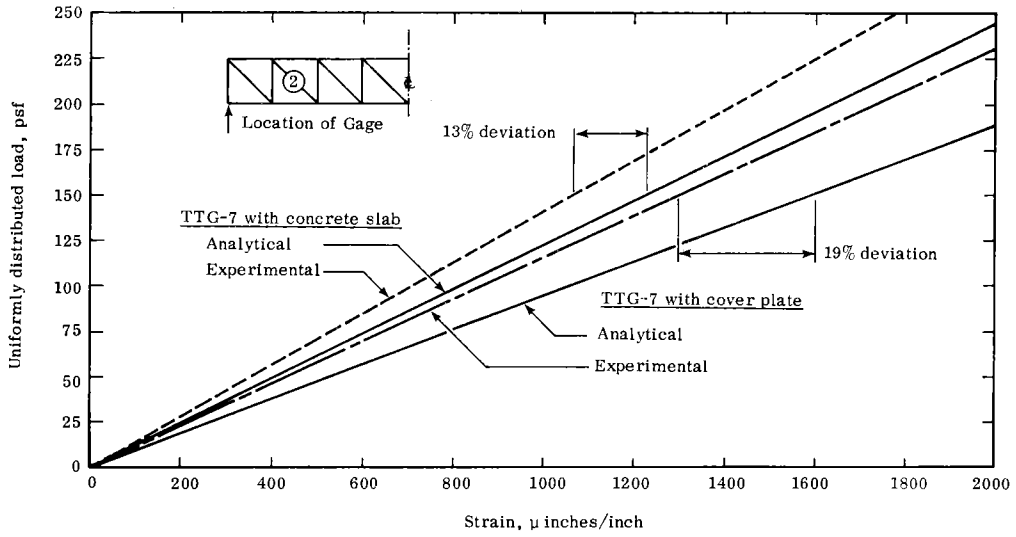

Figure 10. Comparison of analytical and experimental strains in a web diagonal of TTG-7.

FLEXURAL CREEP BEHAVIOR OF GIRDER TTG-6

Flexural creep data were obtained from a single specimen (TTG-6) fabricated with the top plate joint configuration shown in Figure 2. The specimen alone weighed 50 pounds and was loaded with a total of 1,200 pounds of dead weight distributed to the top plate through an air bag for an equivalent uniform load of 150 psf. This loading represents a 50% overload based on a design load of 100 psf and was applied to increase the creep rate. Figure 11 shows the specimen under load in a room in which the temperature was 74° ± 2° F over the test period. Measurements were made of vertical displacements at three panel points and strains in selected elements.

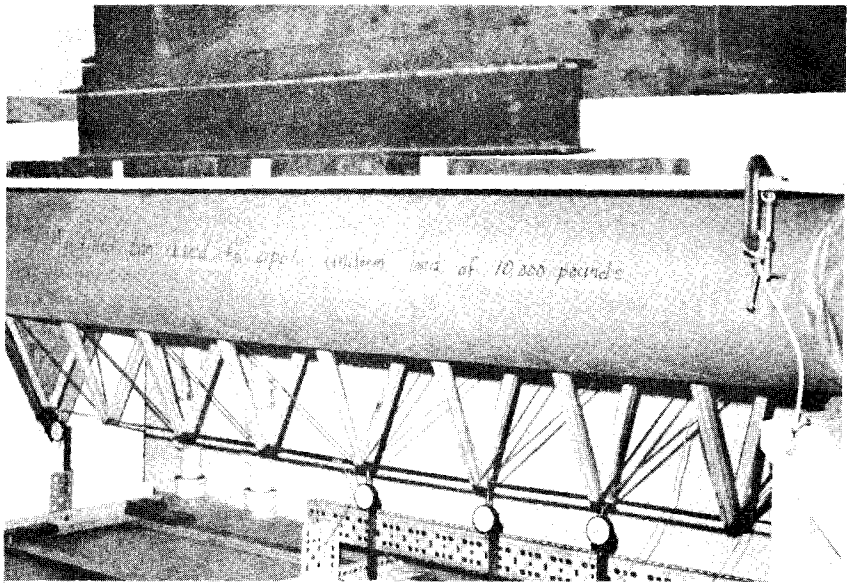

Figure 11. Creep test of TTG-6 loaded to 150 psf.

All deflections were measured with mechanical dial indicators and strains were measured with bonded electrical resistance gages. The 1,200-pound load remained undisturbed on the specimen for a period of 95 days.

Figure 12 presents the deflection data for the center panel point and shows the location of the various gages on the specimen. Except for the elastic deflection values for dial gages 2 and 3, which were smaller, the incremental increases of deflection with time, including the range of scatter, were essentially the same as those for the center gage. These data indicate that all of

the panel points displaced downward the same amount and at the same rate. This indication would imply either a continual redistribution of stresses among the elements, which equalized deformations, or that all of the creep deformation occurred within the end panels. This performance was not anticipated even though the strain gages indicated that the diagonals in the end panels were the most highly stressed elements. No satisfactory explanation can be offered for the magnitude of the scatter of the deflection data. Room temperatures were monitored with the thought that thermal variations might cause reverse movement of the dial indicators, but no correlations could be established between the deflection readings and the slight temperature fluctuations which occurred.

Unfortunately, the strain data offered little clarification of the deflection behavior, because the strain indicator ceased to function after five days into the test program. Because of the nature of the indicator malfunction, all of the data must be considered suspect. Nevertheless, the data indicated that there was a stress relaxation (of approximately 2.5%) in the lower chord elements of the center panels and increasing strains in both diagonals, the greater (6.8%) occurring at gage location 1. The deflection recovery characteristics of the member appeared quite good. Essentially all of the elastic displacement was recovered and approximately one-half of the creep after a period of 27 days.

Should further study confirm that nearly all of the flexural creep deformation occurs in the end panels, the size of the diagonals in these panels can be increased to offset the long-term creep effects. It should be noted that the highest elastic stress computed from strain measurements was approximately 9,060 psi in the end panel diagonal. If the rate of creep shown in the secondary region remained constant, a deflection of approximately 0.3 inch would occur in ten years. The effect of the movement of joints was an unknown factor and may have contributed significantly to the overall deflections. Additional observations of the creep phenomena would be required to fully characterize the anticipated behavior of the girder. The load-creep relationship would be of particular interest to obtain performance data at anticipated service loads.

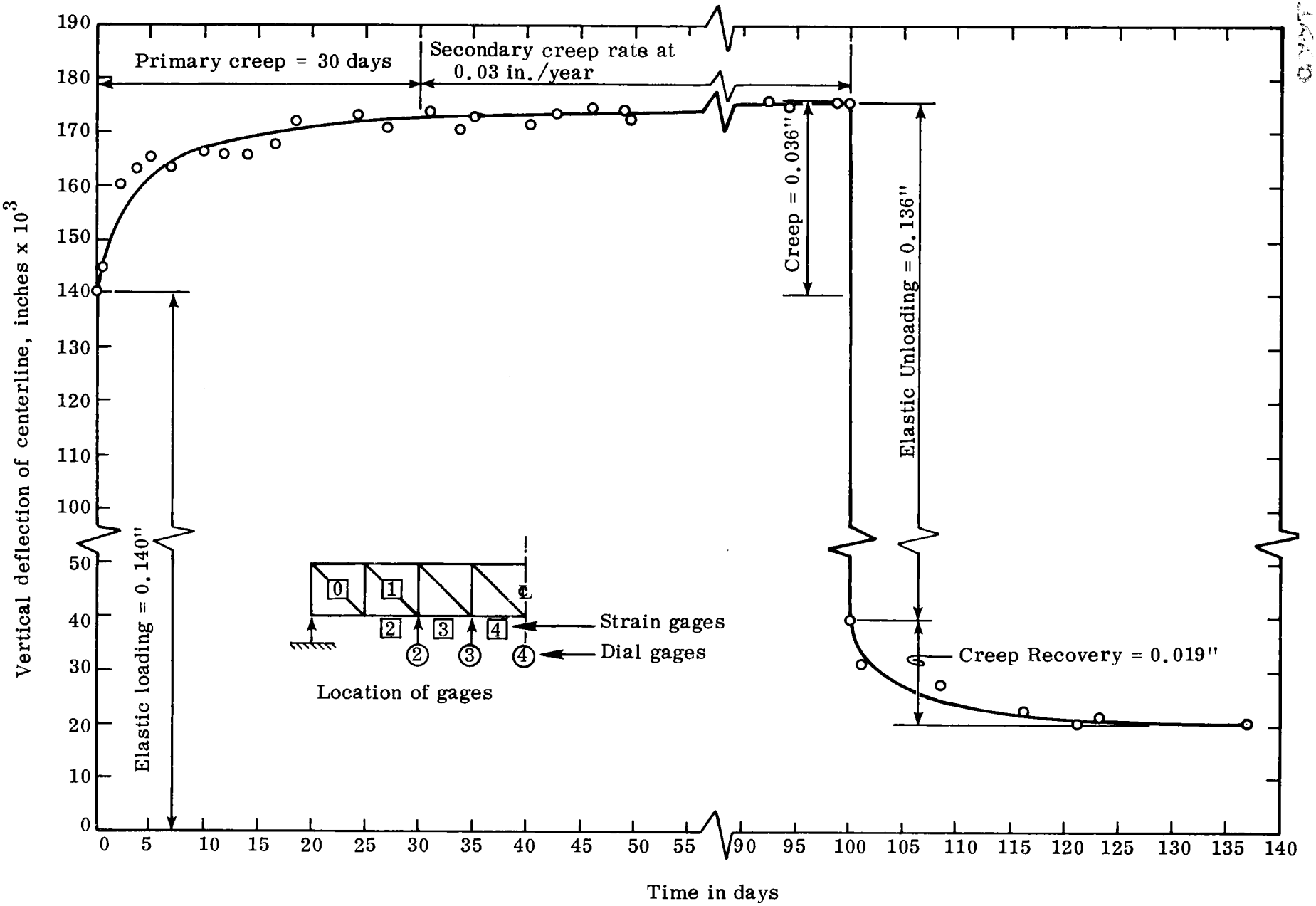

Figure 12. Deflection of centerline of TTG-6 under constant load of 150 psf.

PERFORMANCE OF TRISECTIONAL STRUCTURE (TTG-8)

Fabrication

A test specimen consisting of three members identical to those of TTG-7 was fabricated and designated TTG-8. A single cover plate 4 feet wide by 8 feet long by 1/4 inch thick was bonded simultaneously to the top plates of the individual girders to provide a connection for the three units. No other lateral connections were made to tie the units together since it was intended to observe the independent action of each girder under different load arrangements.

No particular problems were encountered during the fabrication of the total structure. The surfaces of mating plates were sanded, cleaned with alcohol, and coated with the polyester resin used in the winding operation. In order to apply pressure normal to the top plates of the girders without deflecting the members, the cover plate was placed on a resilient support and the girder plates bonded with the girders in an inverted position. Pressures of unknown magnitudes were obtained by dead weights placed at various points over the structure (see Figure 13). Visual inspection of the joint before and after load testing revealed no defects. No other inspection methods (e.g., ultrasonic) were used to evaluate the continuity of the bonded joint. Figure 14 is an oblique view of the completed three-sectioned structure prior to load testing.

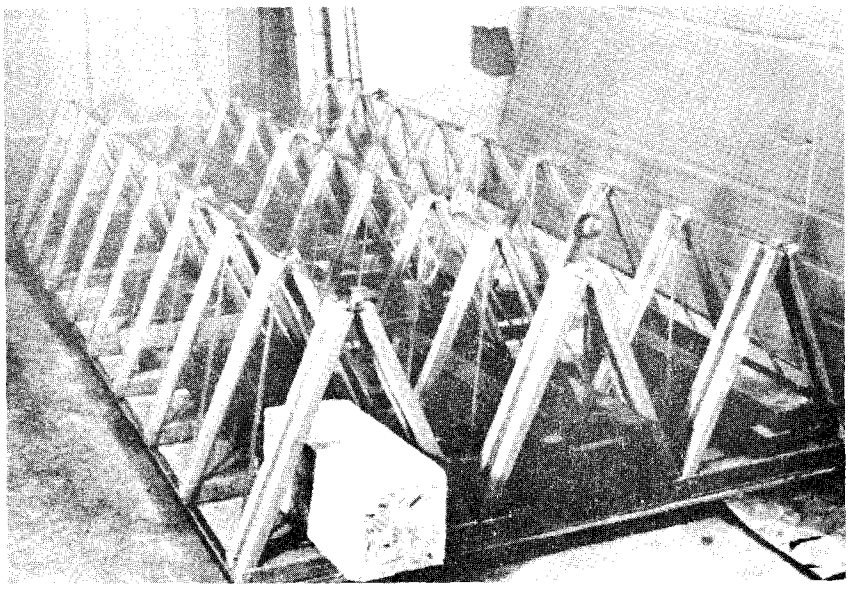

Figure 13. Joining procedure for bonding the cover plate and top plates of TTG-8.

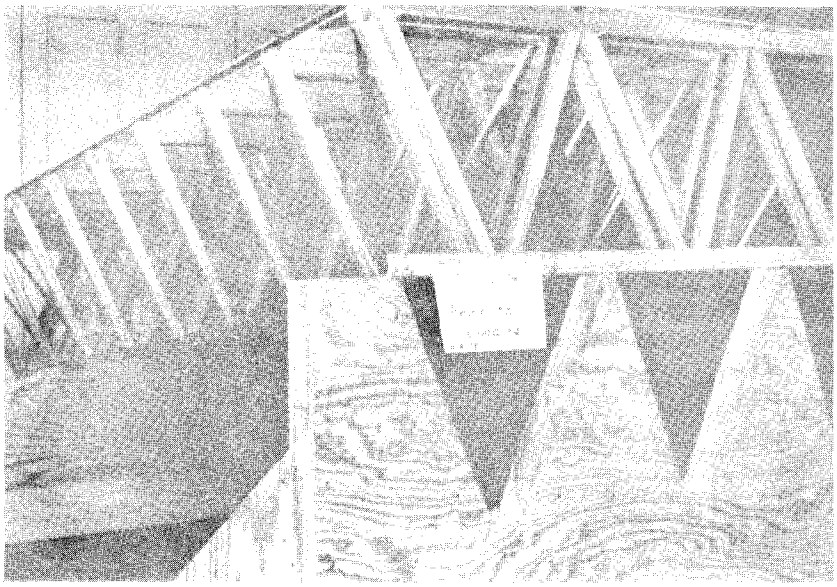

Figure 14. Oblique view of TTG-8 showing completed structure prior to testing.

Load Tests

Load tests were conducted with TTG-8 in the same manner as described previously for other test specimens. Strain and deflection instrumentation was arranged to facilitate data production by utilizing the geometric symmetry of the structure. Accordingly, 17 bonded strain gages, 9 vertical deflection indicators, and 2 horizontal deflection indicators were used for displacement measurements. The locations of the strain gages and dial indicators are shown in Figure 15.

Vertical static loads only were applied to the top plate during the test series. The various load arrangements were as follows:

1. Uniformly distributed load over one edge section only.

2. Uniformly distributed load over the two edge sections only.

3. Uniformly distributed load over the center section only.

4. Uniformly distributed load over the entire surface.

5. Uniformly distributed load over the two-end panels on both ends of the structure.

6. Line load (4 inches wide) transversely across the structure at the centerspan.

7. Line load (4 inches wide) transversely across the member at the second panel position on one end only.

It was necessary to use two air bags to cover the entire surface of the structure for load arrangement 4. However, due to the curvature of the inflated bag, a 9-inch wide strip along the centerline of the structure was not in contact with the bags. Therefore, the conditions of a uniformly distributed load over the entire surface was not actually achieved for load arrangement 4. Figure 16 shows a typical uniform load test in progress.

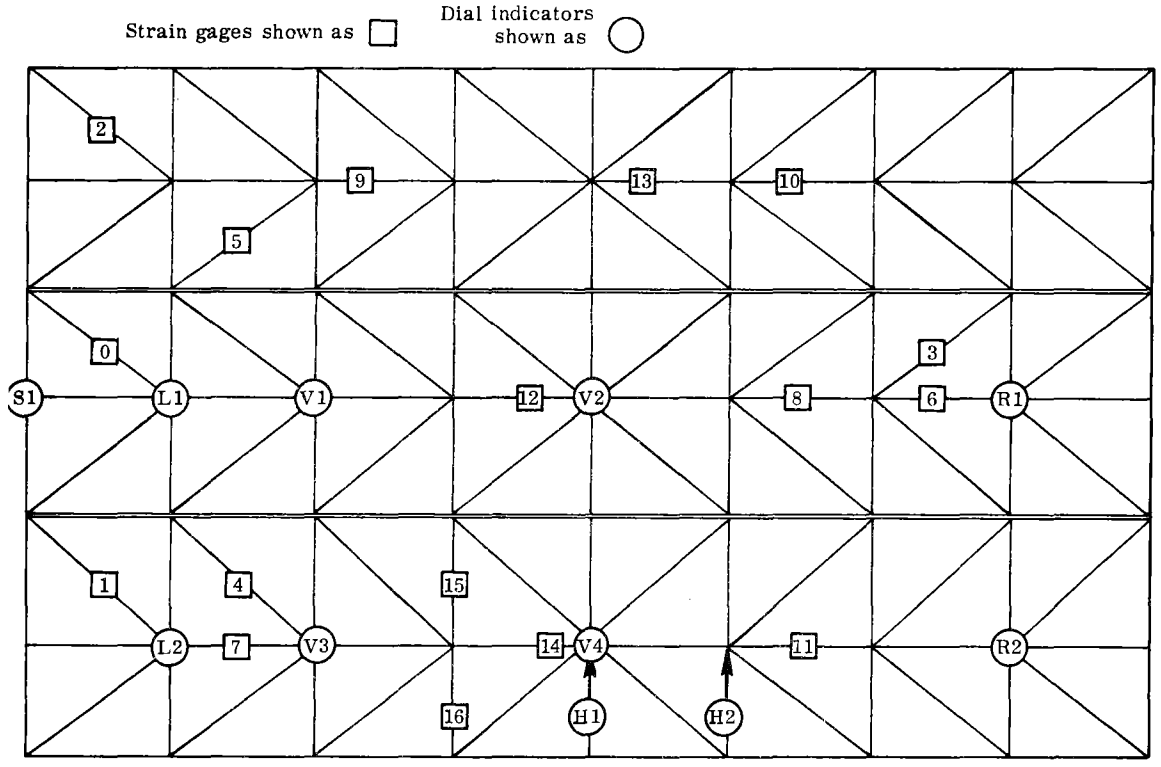

Figure 15. Schematic plan of TTG-8 showing positions of indicators and gages.

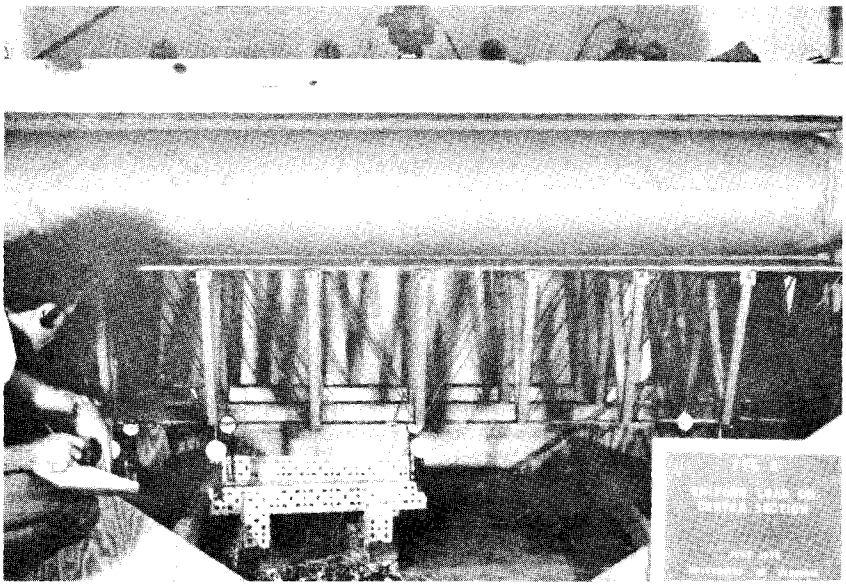

Figure 16. Typical load test of TTG-8 using an air bag to provide a uniformly distributed load.

Failure Mode (Buckling of Web Elements)

No ultimate load was determined for TTG-8. A maximum total load of 3,200 pounds was distributed over the entire surface for an equivalent uniform load of 100 psf. A maximum unit load of 210 psf was applied for the condition of the center section only being loaded. Higher loads were not applied to prevent possible damage to elements before all investigations were completed. No damage nor distress of any kind was observed in any of the joints or elements, but several loud cracks were heard as the higher loads were reached.

Nonsymmetrical loading of the structure caused elastic buckling of some of the diagonal elements at relatively low loads. This behavior was expected due to the reversal of the panel shear force for loads extending only partially over the end panels. When a single edge section was loaded, buckling of some elements was observed in the unloaded edge section. This behavior suggested the presence of torsional moments transmitted through the cover plate. The buckling observations are discussed further in the analytical section. While indicative of a condition of instability, all evidence of buckling disappeared upon removal of the load and did not impair the performance of the structure in subsequent tests.

Experimental Deflection Measurements

Vertical Deflections

Vertical deflections of lower panel points were made at the positions shown as L and V in Figure 15 for the various load arrangements listed previously. Comparative deflection data are shown in Figure 17 for four of the loading conditions applied over the indicated sections for the full length of the member. Figure 17(a) compares the deflections of the loaded section or sections with those of the unloaded section or sections at the center panel points (V2 or V4) and at the second interior panel (V1 or V3). Figure 17(b) shows the deflection profile for the center panel points for the three sections. All of the data shown are for deflections of the indicated panels relative to the corresponding first panel points (L1 and R1 or L2 and R2). Relative deflections were shown to eliminate the effect of settlement of the ends of the structure in the supports. The actual net deflections were therefore somewhat larger than the values shown in Figure 17. Efforts were made to monitor movement at the supports, but most of the observations were not considered reliable. In general, the measured deflections were linear with the magnitude of applied loads. Data will be presented to indicate this linearity in the following section which describes the analytical study.

Several interesting behavioral characteristics were revealed by the deflection measurements.

1. The inability of the cover plate to transmit loads from the loaded to the unloaded section may be deduced by observing that the deflections of the loaded sections for load arrangements 1, 2, and 3 were very nearly the same. This result indicates that the cover plate had little load transfer effect and that the sections behaved almost independently of each other, even though the total load on the structure for arrangement 2 was twice that for arrangements 1 or 3. Obviously, the effectiveness of the cover plate in transferring loads from one section to another would vary with the stiffness of the plate, and in the case of a bridge deck with a concrete wearing surface several inches thick, better transfer characteristics should be developed.

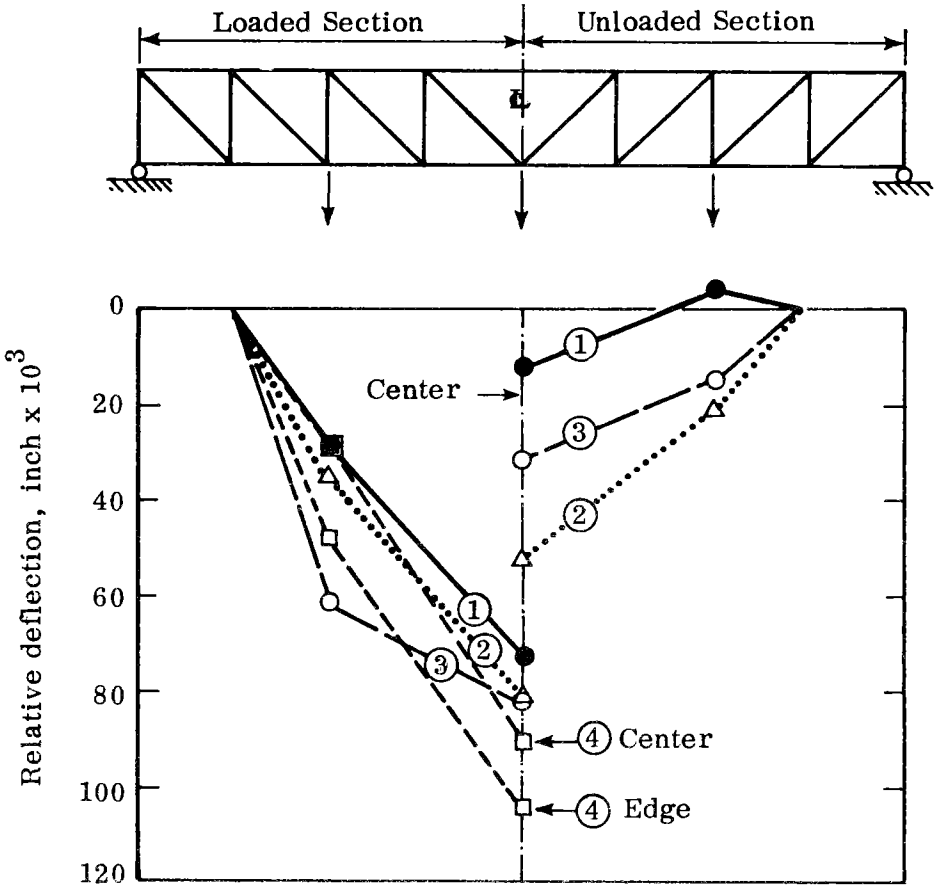

(a) Comparison of deflections along the length for loaded and unloaded sections.

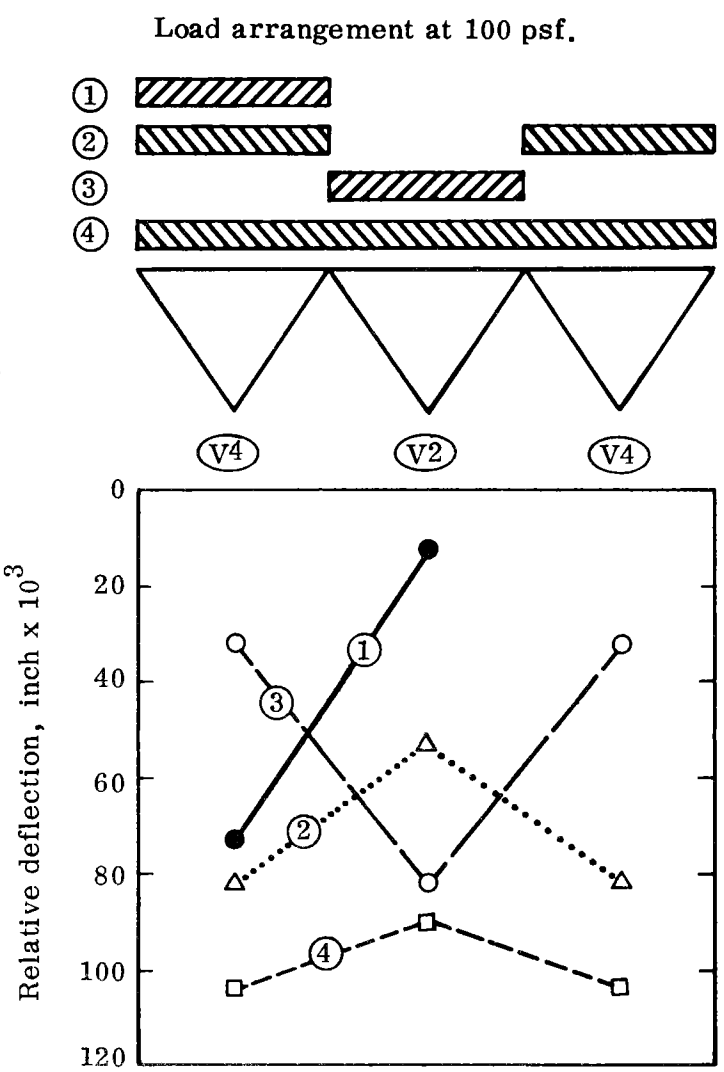

(b) Deflections along the width at midspan.

Figure 17. Vertical deflection of TTG-8 for various arrangements of a 100 psf load.

2. The sensitivity of the structure to load distributions was apparent from arrangement 4. As stated previously, there was a separation of the air bags at the center of the middle section which amounted to approximately one-half of the width of the section. Therefore, the similarity in the shapes of curves 2 and 4 in Figure 17(b) wherein the center section deflected less than the edge sections, was to be expected. Figure 17(a) indicates that the reduced deflection of the center section occurred along the entire length of the structure. It is also of interest that the total load on the structure was 50% more for arrangement 4 than for 2, but the deflections of the loaded sections of arrangement 4 were only 27% higher than those for 2.

3. The principle of superposition appears to hold reasonably well when deflections due to combinations of load arrangement are used to check equivalent loading. For example, the sum of the loads for arrangements 2 and 3 should equal that for arrangement 4. The sum of the deflections in the edge span due to 2 and 3 equals 0.114 inch which compares favorably with 0.104 inch due to 4. The center span comparisons are not as close due to the unloaded portion of the center section. Agreement between arrangements 1 and 2 is also good with deflections of 0.073 for 1 versus a value slightly greater than 0.082 for 2. (The unloaded edge section deflection was not measured for arrangement 1.) Verification of the applicability of superposition was considered important because this principle was used for the analytical study which will be discussed later.

4. The presence of torsional couples, or warping of the structure, due to unsymmetrical loading of arrangement 1 was suggested by the negative relative deflection in the unloaded center section. The numerical value of the deflection was small and may have resulted from shifting of the dial indicator or an unusual movement of the support frames. However, if accurate, this behavior represents an undesirable characteristic and will be treated more fully in the discussion of the results of the analytical study.

The structure responded to the symmetrical transverse loads as anticipated. The uniformly distributed load over the four end panels produced very little difference in the relative deflections between the panel points discussed previously. The midspan line

load produced differential deflections along the length of the structure and a net center span value of 0.133 inch at a total load of 1,200 pounds. This value compares with a value of less than 0.100 inch for a load of 100 psf distributed over the entire surface (3,200 pounds total). The nonsymmetrical transverse line load, placed at gage positions V1-V3 (Figure 15), caused buckling of a number of web elements at loads of several hundred pounds.

Horizontal Displacements

The horizontal displacements of lower chord panel points were measured at the positions shown as H1 and H2 in Figure 15. The purpose of these measurements was to ascertain the magnitude of the horizontal displacements which occurred with load and to provide information relative to the need for lateral ties or bridging between individual sections. Results of the more interesting of these measurements are shown in Figure 18. Movement of the edge section toward the center section was designated as minus and movement away from the center section was designated as plus to correspond to the sign of the stress which would exist in rigid lateral connections (if used) between sections.

The data shown are absolute displacements and it is presumed that there was no lateral movement of the center section for the symmetrical loads shown. Therefore, the linear displacements of the edge sections were due to rotation of the section in response to torsional couples transmitted through the cover plate. The direction of the displacements confirmed intuitive predictions, but the magnitude of the displacements for load arrangement 4 was larger than anticipated considering that the load covered a portion of the center section. Even if reduced by one-third to correspond to the total load applied for arrangement 2, the displacements would still about equal those for arrangement 2. Considerable movement was observed for load arrangement 3, which emphasized the strong influence of the cover plate in transmitting a torsional couple between sections. In comparing the vertical and horizontal displacements for this loading (see Figure 17), it is noted that the horizontal movement was approximately three times that of the vertical. Time did not permit the installation of lateral connectors between the sections to investigate the magnitude of forces required to prevent free horizontal movement of the sections. However, it appears that rigid ties may be required to maintain lateral stability between the sections if heavier cover plates or wearing slabs are not effective in eliminating the horizontal movements. While several efficient schemes for lateral restraint could be used, one would be to attach a thin plate to the lower chords that would cover the entire bottom surface of the structure. The use of a solid plate would also be desirable in field installations to protect the small, stranded elements from possible vandalism, environmental vectors, nesting birds, and other sources of damage.

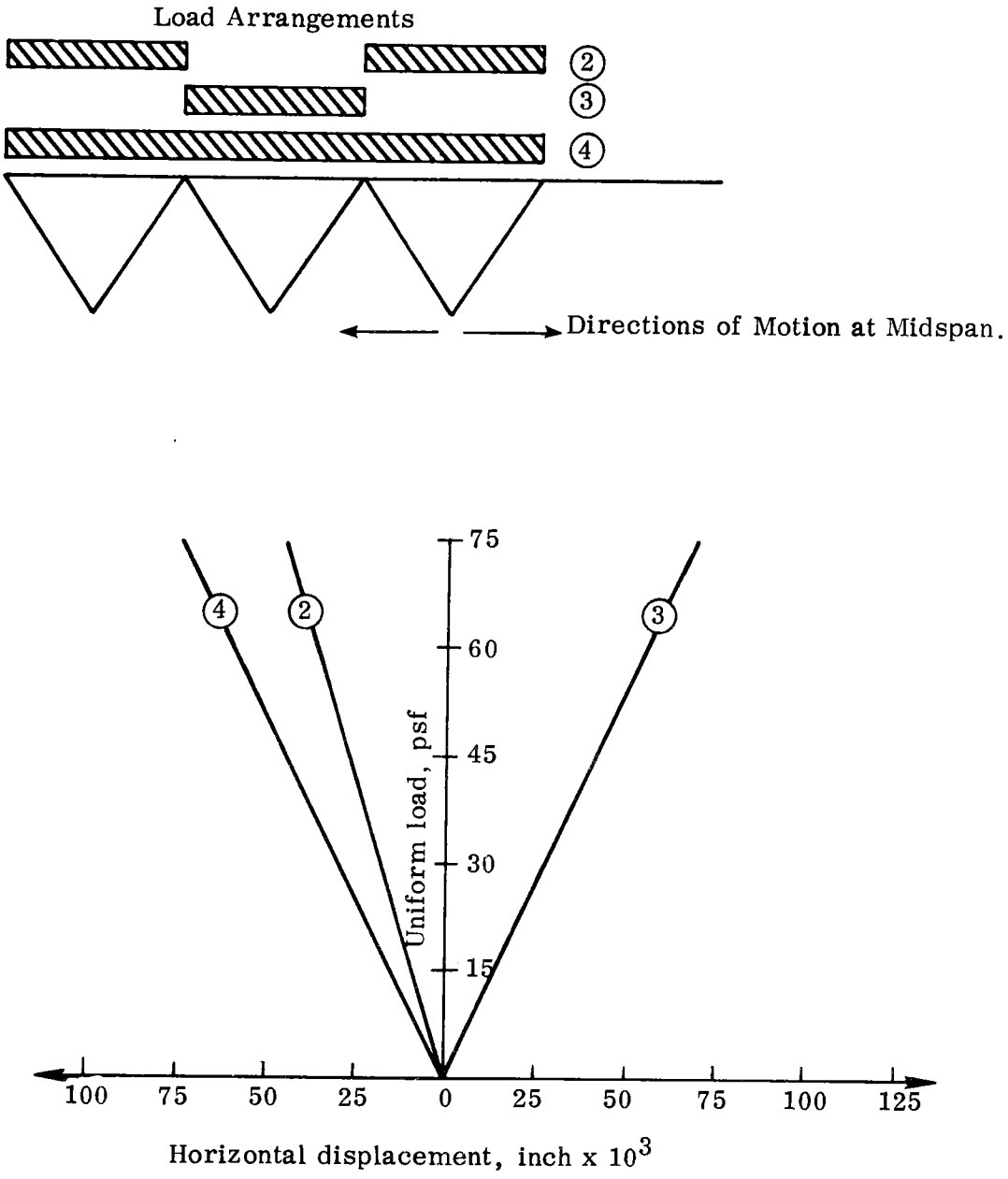

Figure 18. Horizontal displacements of edge section for various load arrangements.

Experimental Strain Measurements

In general, strains measured with the bonded electrical resistance gages were linear with load as shown for TTG-7 in Figure 7. The location of the gages as shown in Figure 15 provided a check on the symmetry characteristics of the structure and the load distribution. In general, there was good agreement between symmetrically located gages for applicable load conditions. All gages were mounted on tensile elements except 15 and 16, which were mounted on the tubular stiffeners. Gage 15 indicated small negative strains and gage 16 indicated nothing. It is believed that these gages were subject to strains resulting from combined axial and bending stresses and therefore did not provide a true measure of the axial strains involved. Future data from these gages will have to be corrected for the flexural action of the stiffeners.

Figure 19 shows the strain magnitudes of selected elements for distributed loads of 100 psf. The center two bars in the figure are for strains in web and chord elements for the loaded sections and the outer two bars are for strains in the adjacent unloaded sections. All sections were loaded in arrangement 4. Ideally, all elements in the loaded sections should be strained equally to achieve greatest efficiency of material usage. No attempt was made to optimize the areas of elements for strain in TTG-8, so the measured strain differences were not considered a design deficiency for this experiment.

The superposition of strains for some of the load combinations coincide reasonably well but some do not. In particular, the strain in gage 1 for load arrangement 3 was irregular, possibly due to horizontal movement occurring near that gage position. This load test was repeated four times with the same disparity indicated by gage 1 in Figure 19. On the other hand, the sum of the strains for gage 0 from load arrangements 2 and 3 is 730 u-inches which compares favorably with 660 u-inches read directly from load arrangement 4. Comparison of the superimposed values versus the direct readings for the chord elements for the same load arrangements are in better agreement, i.e., 525 versus 500 u-inches for gage 14 and 415 versus 378 u-inches for gage 12.

Comparisons of strains between load arrangements 1 and 2 show the anticipated behavior of gage 12 (twice the strain for twice the load) and nearly the same strain values in gages 13 and 24. The latter readings imply that a load in one edge section produces little strain in the elements in the unloaded edge section.

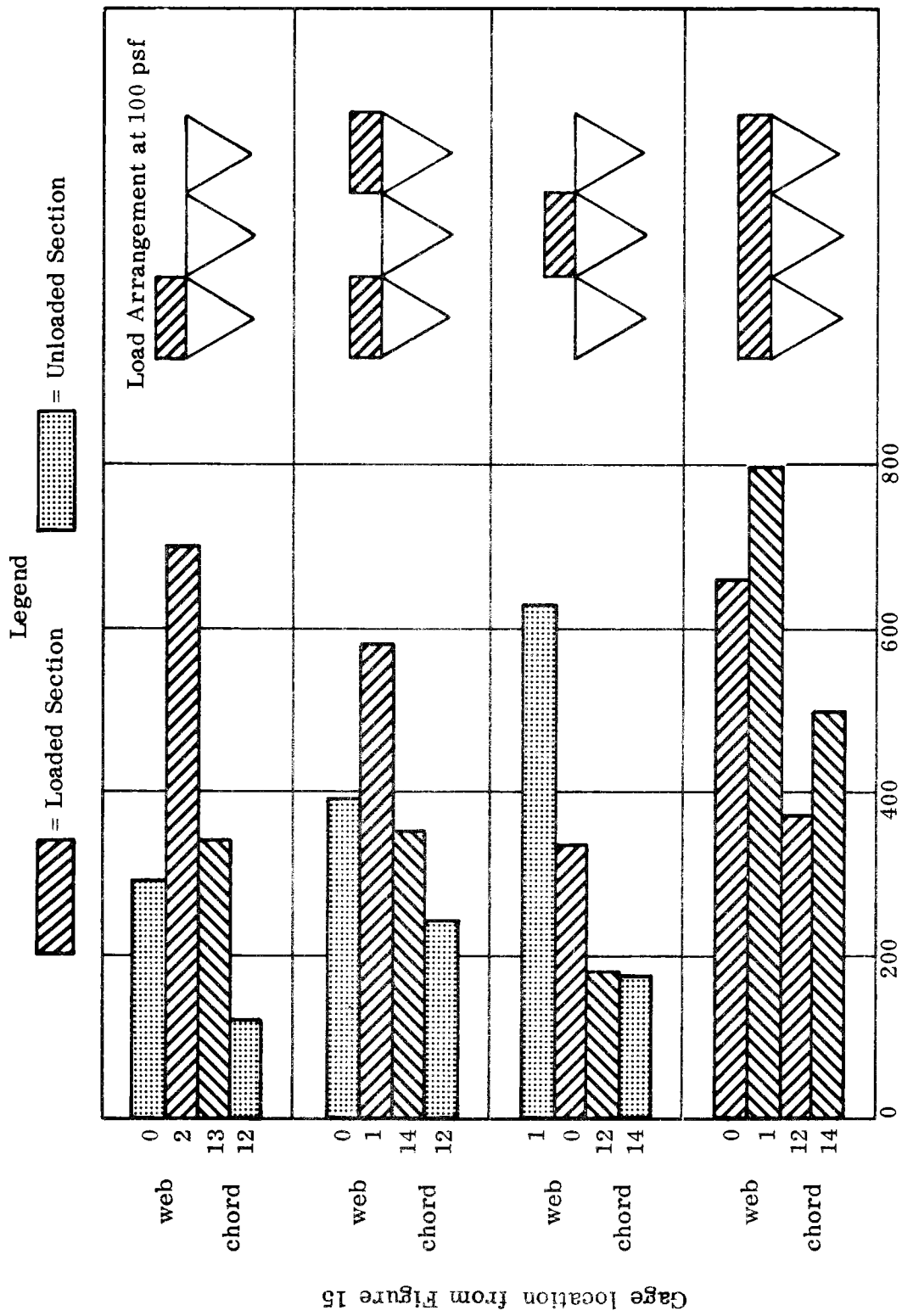

Figure 19. Strains in selected web and chord elements for various load arrangements.

This characteristic of the structure was verified by readings in gage 14 versus those for gage 13 for load arrangement 1, in which strains in gage 14 were between 5% and 10% of those in gage 13 for load magnitudes up to 150 psf. Agreements of strains for the web elements were not as good. Gages 0 and 1 were located in end panels of the sections and therefore were more sensitive than the gages in the chord elements to slight differences in the external supports or strand anchorage. It is believed that most of the observed discrepancies in the web element strains may be attributed to these factors.

The maximum observed strain during all of the load tests was 1,200 u-inches/inch in gage 1 at a load of 200 psf. When multiplied by the elastic modulus of 7×10^6 psi for this member, the maximum tensile stress developed at the applied load of 200 psf was 8,400 psi. This value compares to 10,500 psi for the single unit member, TTG-7 gage 1, at the same applied load.

Analytical Studies

The computer program prepared for the analysis of the multisectional structure provided for both symmetrical and nonsymmetrical load applications normal to the top surface of the structure. Loads could be point or line or uniformly distributed over the plate in any combination attainable by the principles of superposition. However, since only one-fourth of the entire structure was used for the analysis (47 deformable elements and 69 displacement nodes), all computations required geometric symmetry of the structure about both longitudinal and transverse centerline axes. The program did permit removal of redundant elements from the analytical model to investigate the effect of a buckled element (none of the tensior strands could develop compressive forces) upon the redistribution of strains and deflection throughout the structure. Because of the ease of obtaining a complete analysis of the structure, a number of partial loading conditions, in addition to those described for the experimental studies, were investigated mathematically.

Comparison of Analytical and Experimental Results

Figures 20 and 21 show comparisons of typical predicted and experimental measurements for deflections and strains, respectively. The data presented in these figures are typical of the findings in general and were selected to demonstrate the linear deformation behavior of the structure as well as to indicate the nature of the deviations between the analytical and experimental results. Overall, deviations for the deflection measurements ranged from nearly zero up to 20% with a mean around 12%, whereas the deviation for the strains ranged from nearly zero up to 30% with a mean around 20%.

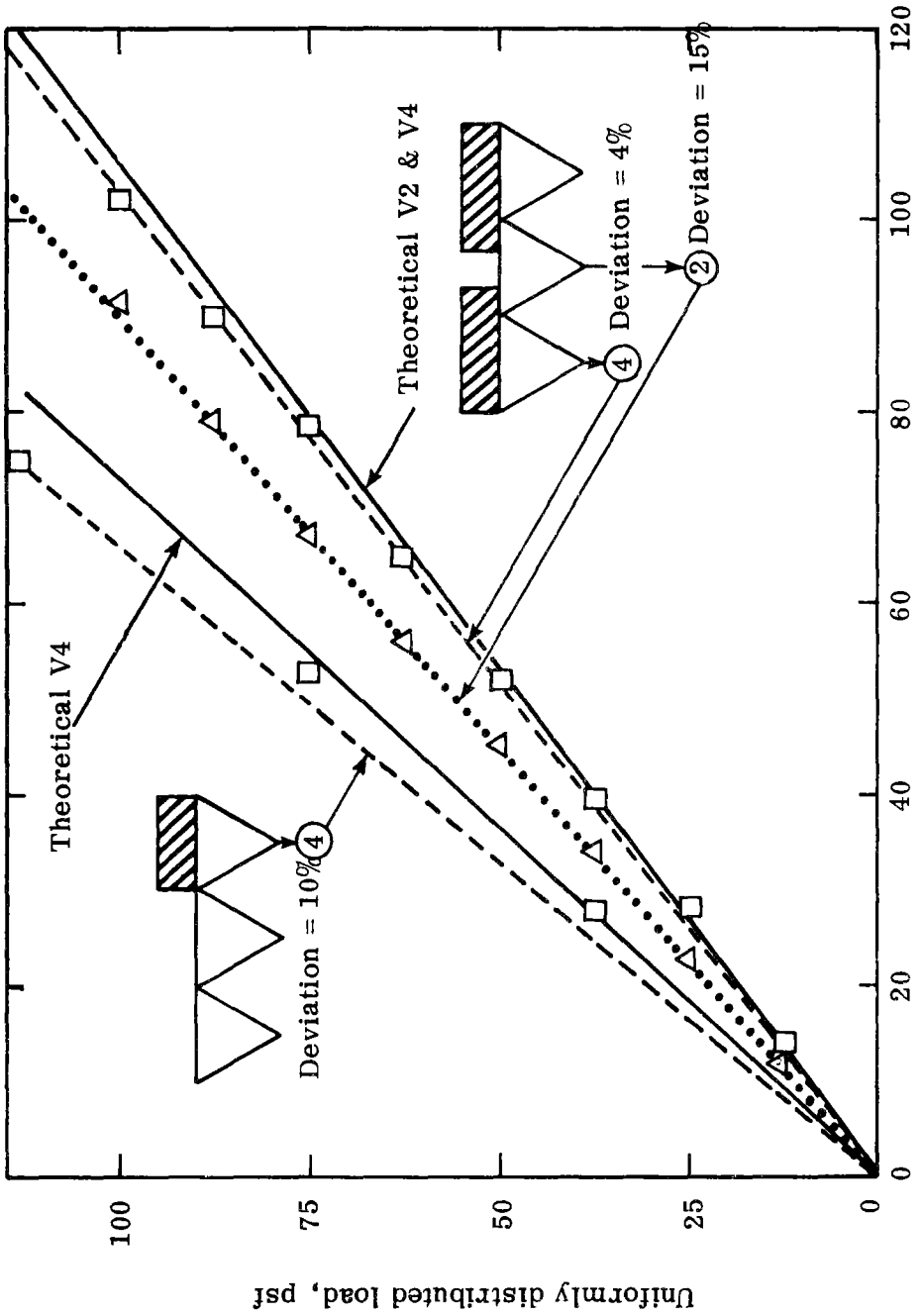

Figure 20. Typical theoretical and experimental deflection at midspan for two load arrangements on TTG-8.

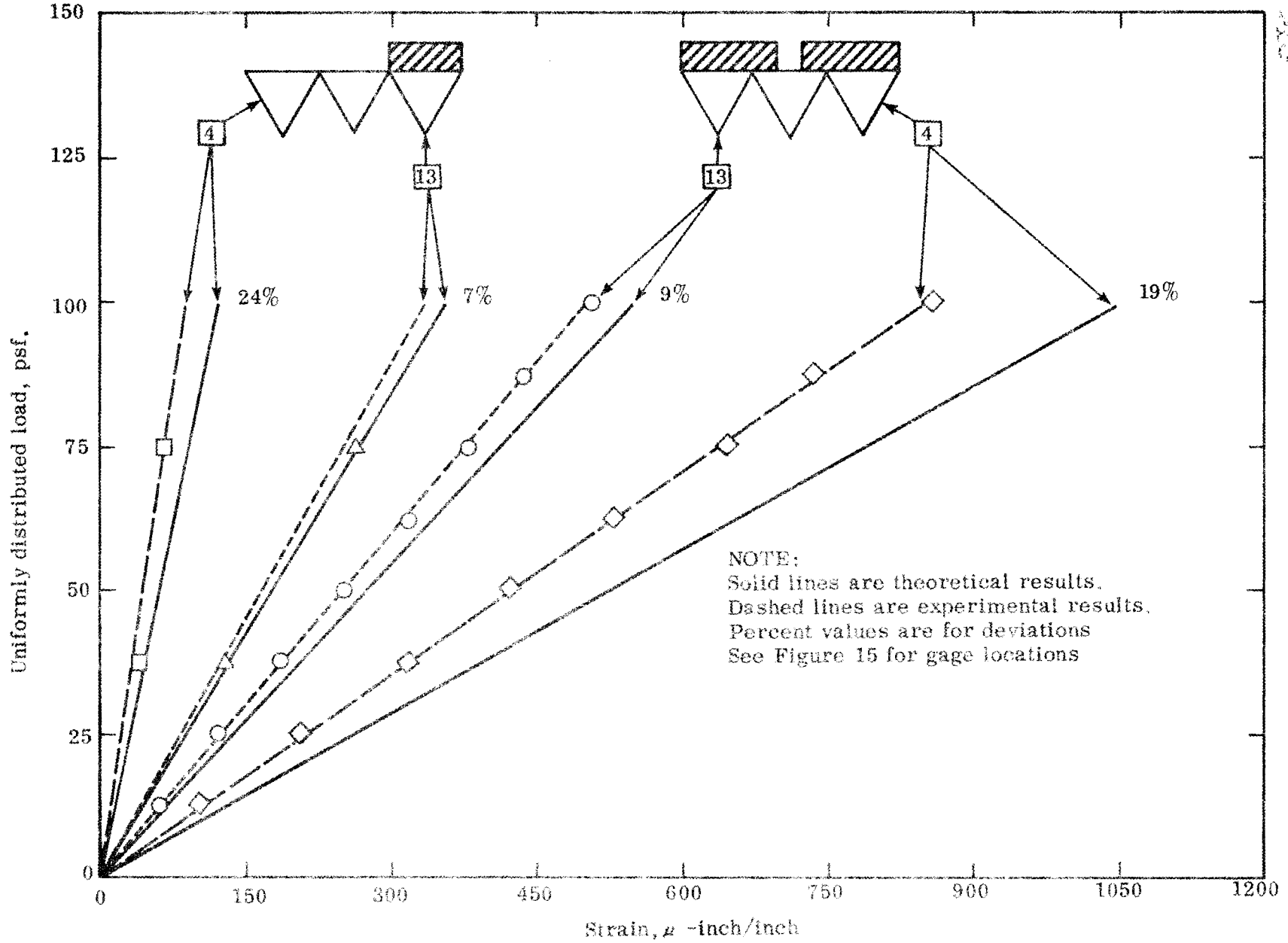

Figure 21. Typical theoretical and experimental strains for two load arrangements on TTG-8.

The deviations of strains in the web diagonal elements, as a group, were higher than those for the lower chord elements. In nearly every element, whether a web diagonal or a chord, the experimental value was less than that predicted by the analysis. This was true for both strain and deflection measurements. From a behavioral standpoint, these results indicate that the joints undoubtedly transmitted some moment and provided more stiffness to the structure than was assumed for the analytical model. From a design standpoint, the consistency of the higher predicted values would permit an empirical adjustment to the theoretical model to account for the indeterminant stiffness of the joints and thereby bring the theoretical and experimental values into closer agreement. A comprehensive study of empirical modification to the analytical model was not made in view of the physical modifications which should be made to reduce relative lateral movement of the sections under loads. These modifications would change the stiffness characteristics of the structure and produce different sets of data from those obtained in the current investigation. Also, a time limitation for the completion of the major goals of the project precluded interesting studies of this nature.

Partial Loading and Buckling of Elements

It was mentioned previously that some of the web diagonal elements buckled when a load was applied over a portion of the plate surface. This was anticipated in view of the single diagonal tension element present in each panel. A number of nonsymmetrical partial load arrangements were studied by means of the computer program to ascertain which tension elements would undergo stress reversal and be subject to buckling.

One experimental load test was conducted to check the analytical results. This test consisted of a live load applied across the structure at the second panel position from an end support. Figure 22 is a plan view of one-half of the structure showing which members were predicted to buckle and which members actually buckled due to the load. Other web elements appeared to retain some tensile stress even though the strains were small. Figure 23 shows the deflection profile of the lower chord in the center section, which clearly indicates an upward movement of the girder. This movement was apparently due to buckling of the top plate in an upward direction between the load position and the support, and occurred when the compressive stress in the plates exceeded the critical buckling value for that element.

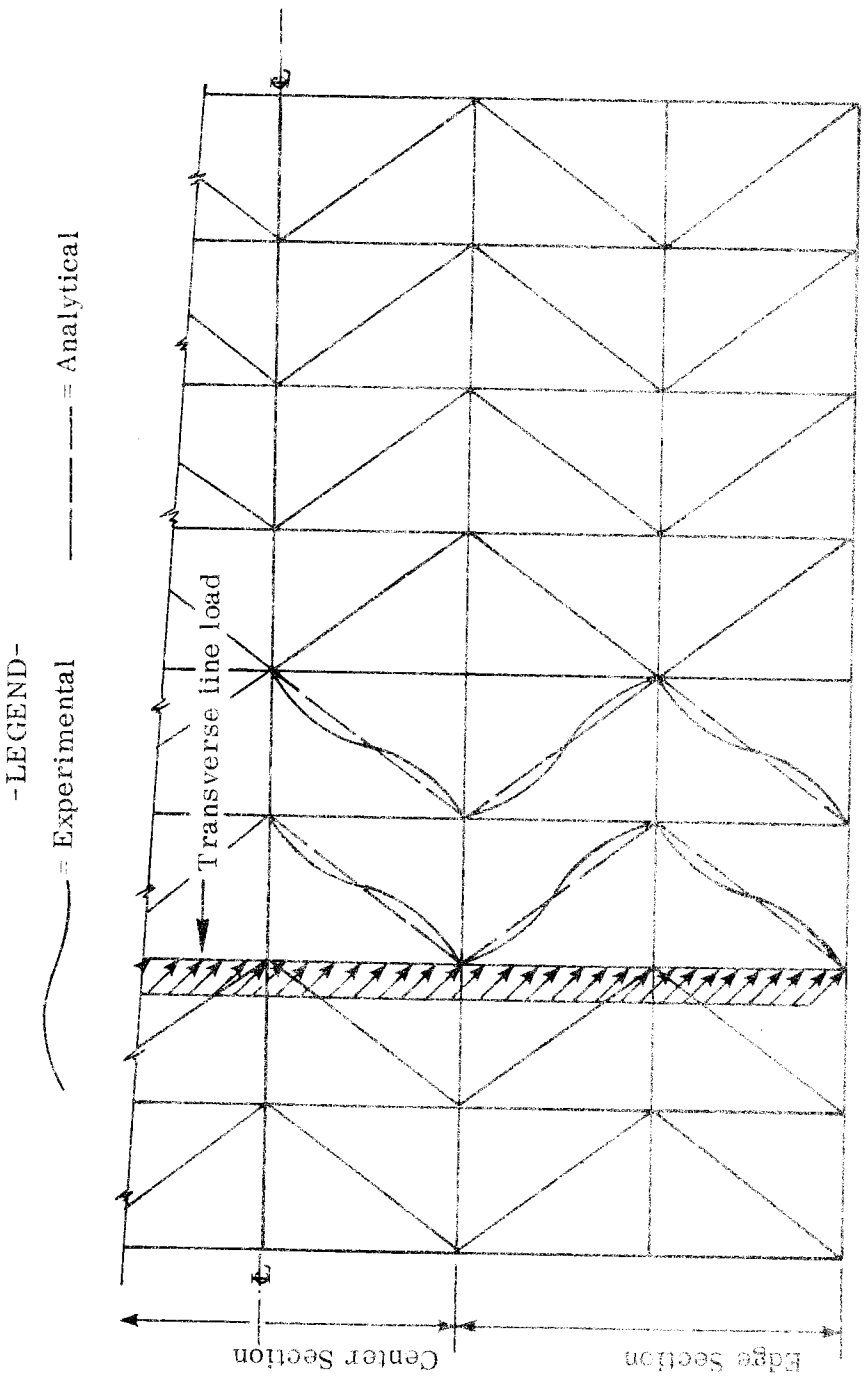

Figure 28. Plan view of one-half of TTG-8 showing elements which buckled due to a transverse line load.

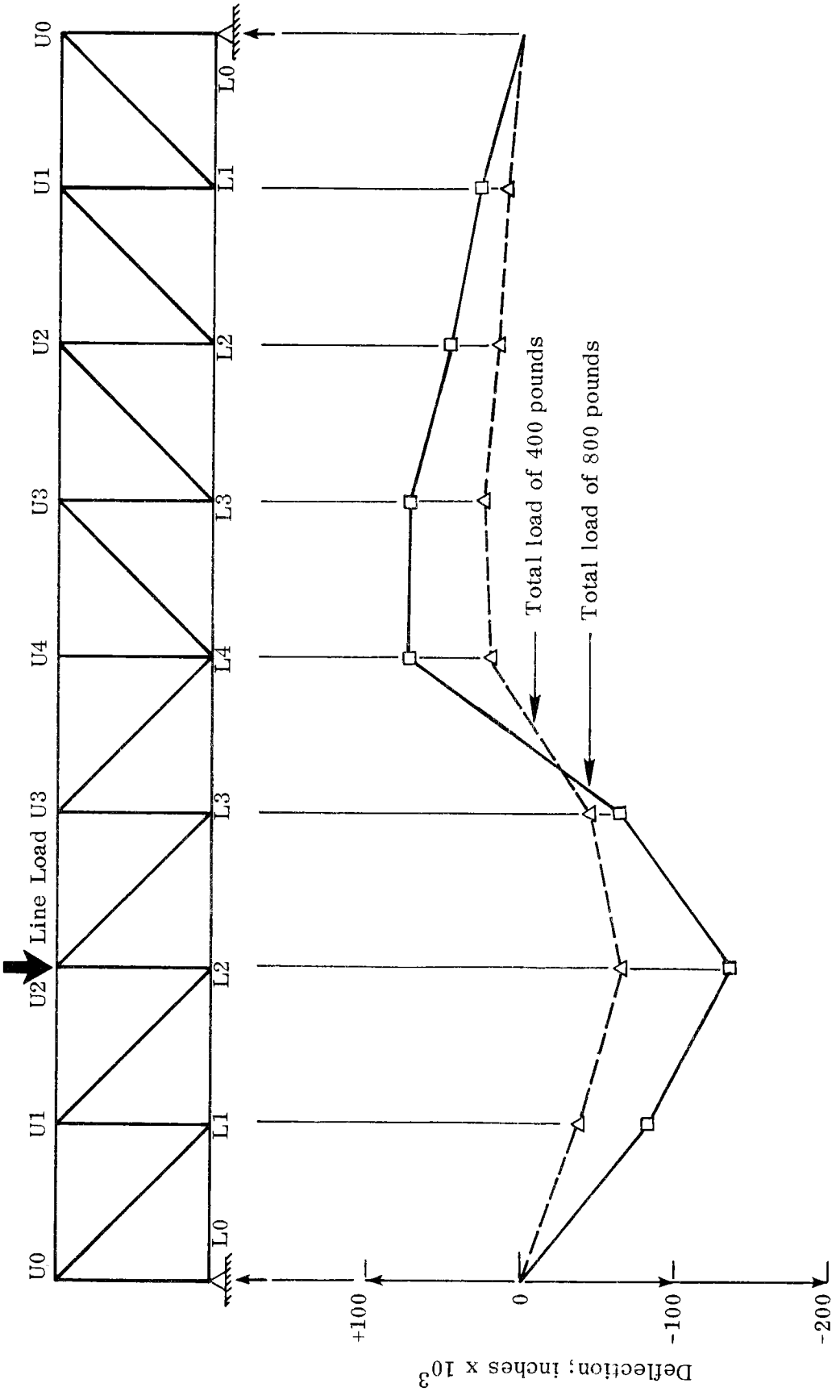

Figure 23. Deflection of center section of TTG-8 due to a line load.

Two steps can be taken to prevent distortion of the panels due to stress reversal. First, cross diagonals could be placed in each panel to develop the requisite tensile forces to maintain panel integrity. Some fabrication difficulties would be anticipated for this procedure. An obvious disadvantage would be the use of additional material and labor to complete the section. Secondly, the dead weight of the structure could be increased by a concrete top slab so that the shear stresses in the panels would not reverse under action of the live load. Certainly a combination of heavier top plates (or slabs) than those used for TTG-8 would be required for the deck of a bridge in service, but unreasonably large dead loads would be required to compensate fully for all possible live load conditions. For example, several arrangements are shown in Table 1 in which the dead load was varied by the depth of a concrete slab with a density of 150 pcf. A live load of 85 psf was used in the computations. No allowance was made for the weight of the structure itself (5.6 psf). Only those elements requiring the higher dead load compensations are included in Table 1. Lower loads would eliminate the buckling of other elements.

It is apparent from the data of Table 1 that a combination of dead weight and cross diagonal web elements in the critical panels should be used to counteract the stress reversal problem. Thus it appears that the use of a reasonably heavy (30 to 50 psf) deck slab of an inexpensive structural material would have the advantage of providing a conventional wearing surface, decreasing live load deflections, eliminating most of the live load buckling behavior, and reducing the vibrational characteristics (yet to be investigated) of the structure. The disadvantages of the heavy deck slab would include added erection time and costs and increased design loads for the overall structure.

Table 1

Dead Load Requirement to Offset Effect of Partial Live Loads at 85 psf

Type of Partial Load	Critical Section/ Element*	Slab Thickness, inches
Uniform load on center section	Edge/U0L1	0.2
Transverse line load at U2 on both ends	Edge/U3L4	0.3
Uniform load over two panels at both ends	Edge/U3L4	0.1
Longitudinal line load at center-line	Edge/U0L1	0.4
Point load at center	Edge/U0L1	0.1
Uniform load on transverse one-half	Edge/U3L4 Center/U3L4	6.5 5.5
Transverse line load at U2 on one end	Center/U3L4 Edge/U3L4	7.3 6.4
Uniform load over two end panels at one end	Center/U3L4 Edge/U3L4	3.4 3.0
Uniform load on longitudinal one-half	Edge/U0L1	0.7
Uniform load on one edge section	Edge/U1L2	0.3

*See Figures 22 and 23 for element locations.

Studies on Configurational Optimization

The present configuration of the trussed girder was based partially on intuitive arguments,[3,4] and as has been mentioned previously, the stress distribution in the elements was not ideal. Therefore, studies were conducted for an optimum configuration which might yield a more economical member. A literature review revealed that little work had been done in the field of optimizing the configuration of unknown topology. The few available reports included the following.

a) A. G. M. Michell's (1904) method for determining the optimum layout of bars in a truss-like continum.[5]

b) Hegemier and Prager's (1968) modification of Michell's problem for which a unique optimal layout can be directly determined without trial and error.[6]

c) Prazer's (1974) method of designing trusses with finite numbers of bars that achieve nearly the same economy of material as the corresponding Michell structures.[7]

d) Dorn, Gomory, and Greenberg's (1964) method of finding the optimum geometric configuration of planar trusses subjected to a single set of loads by starting with a network of possible node locations and a ground structure obtained by interconnecting these nodes, with a linear programming algorithm being used to delete some of the members.[8]

e) Dobbs and Felton's (1969) method for including cases of multiple independent sets of loads and use of a steepest descent algorithm to solve the resulting nonlinear problem.[9]

f) A method proposed by Majid and Elliot (1973) that also starts with a ground structure, and uses some structural principles to forecast the manner in which the numerous members should be deleted.[10]

g) W. R. Spillers'(1975) optimality criterion to find the optimum location of the nodes of a truss with a given topology.[11]

For the same reasons which determined the original shape of the member, it seemed desirable to retain a prefabricated plate as the top chord and a triangular cross sectional shape for the girder.

However, the configuration and areas of web and lower chord elements needed to be optimized. None of the above methods provided a direct, practical solution to this problem.

Optimization methods based on mathematical programming search for the optimum configuration in a purely empirical manner. A set of rules is established which will guarantee a continuous and monotonic decrease in a prescribed objective function without regard to the nature of that function. The path to the optimum is shown, but no predictions concerning the optimum are specified, apart from the criterion that it is impossible or uneconomical to go on. Both the strength and weakness of mathematical programming reside in this formulation: its strength being the generality which this independence of problem type imparts, whereas its weakness arises from no use being made of any characteristics of the problem which would permit a more efficient solution. Therefore, although these methods are well-defined mathematically, they are severely limited by problem size and computational complexity. As the number of variables increases, the number of searches also increases and the computational cost per cycle increases rapidly. This limitation is attributable not only to the greater cost of larger analyses but also to the need to compute derivatives of constraints with respect to all variables.[12]

Therefore, in recent years much attention has been focused on optimality criteria methods where, in direct contrast to numerical search methods, conditions are established on some basis concerning the nature of the optimal design. These criteria provide the basis of a simple recursion relation used for redesign. For these reasons, an optimality criteria method was chosen for this study.

Pederson pointed out that for a single loading condition the optimum truss is a statically determinate one.[13] Therefore, it was thought that starting with a ground structure obtained by interconnecting a network of possible node locations and modifying the areas of elements to satisfy the optimality condition, some elements could be deleted. For a three-dimensional study, only a very small number of node locations could be considered because the number of elements would increase rapidly with the addition of new nodes and quickly exceed the capacity of the computer. Therefore, the study was confined to planar trusses. The resulting truss would then be considered one face of the triangular trussed girder.

A computer program written by Victory Perry[14] was modified to serve these specific needs. It can handle 95 elements and 95 degrees of freedom. The following steps were used to explore an optimum configuration.

1. Given a certain span length, select the number of panels desired and sketch a network of possible node locations in the two-dimensional plane.

2. Interconnect these nodal points such that a ground truss of not more than 95 elements is obtained.

3. Use an optimality criteria method for optimizing the areas of a truss to delete some of the elements. To avoid getting an ill-conditioned stiffness matrix, assign a minimum area constraint of 0.00001 sq. in. rather than zero. Consider elements with this area deleted.

4. Pick the nodal points where most of the remaining elements are clustered, at the same time trying to maintain a Pratt truss configuration by grouping some elements together.

5. Select the width and the thickness of the top plate.

6. Analyze the resulting structure using a three-dimensional finite elements method and scale the areas of web and lower chord elements such that the largest deflection of the structure is equal to the maximum allowable deflection.

7. Repeat the procedure for a different number of panels and calculate the volumes of elements.

These steps were tried for the design of girders 8 feet long with 6, 8, and 10 panels and girders 30 feet long with 8 and 10 panels. A uniformly distributed load of 100 psf on the top plate was used in all determinations. The iterations could not be carried far enough in any of these combinations to reduce the ground truss to a statically determinate one. However, in all cases, the heavier elements were clustered around one node in each column of nodes, which indicated the favored node.

Figures 24 and 25 show the different steps in the design of the 8-foot, 10-panel member. Figure 24 is the ground truss of 91 elements and 26 nodes. The same ground structure but with different dimensions was also used for the design of a 30-foot,

10-panel member. In order to consider a more general network of elements and nodes, the geometric symmetry of the structure and loading arrangements were utilized. Figure 25 shows the final shape of the plane truss with these nodes. The elements shown are the sums of the areas of similar elements grouped together.

The top chord elements of the plane truss obtained by projecting the girder onto a vertical plane were much heavier than the web and lower chord elements. To make sure that the web and lower chord areas did not decrease to an unrealistic value, large minimum area constraints were used for these elements. Because of this, the areas reached their minimum limit at the end of the first computational iteration and therefore were inactive for the remainder of the iterations. Thus the width and thickness of the top plate did not affect the results until step 6 of the procedure outlined above. At this point, widths of 16 inches and 48 inches and thicknesses of 0.5 inch and 2 inches were selected for the top plates of the 8 foot and 30 foot long members, respectively. The resulting structure was then analyzed in three dimensions and the areas of web and lower chord elements increased proportionally until the largest deflection of the member became 1/1000 of the span length. In the 8-foot, 10-panel girder, some of the diagonals developed compressive stresses; but since they were incapable of carrying any compression, they were eliminated at this point. The final design of the 8-foot, 10-panel member is sketched in Figure 26.

In a comparative study, the areas of web and lower chord elements of the configuration of TTG-7 were computed by the optimization procedure. The idealized areas along with the actual areas of TTG-7 are presented in Table 2. Volumes of the web and lower chord elements of the several girders were calculated and are summarized in Table 3. It is evident that a significant reduction in volume of material was achieved in going from the actual areas of TTG-7 to the optimum areas for the same span length. Conversely, for the same volumes of material used in the present configuration and the optimized versions of TTG-7, the maximum deflections should be substantially reduced in the optimum shape.

The practical aspects of fabricating an optimized configuration have not yet been explored.

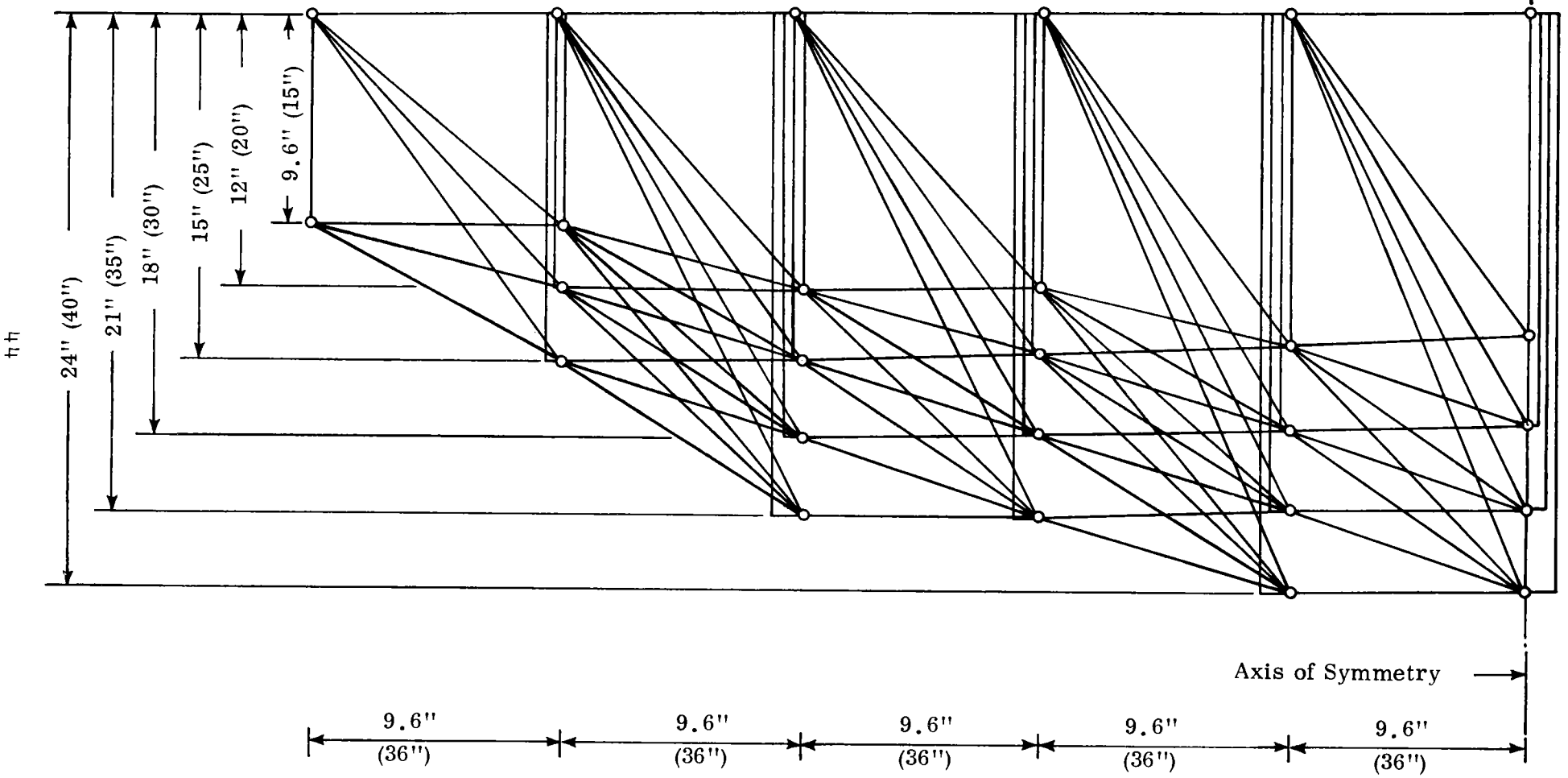

Figure 24. Ground truss for the 30-ft., 10-panel and 8-ft., 10-panel designs. Dimensions in parantheses are those for the 30 ft. member.

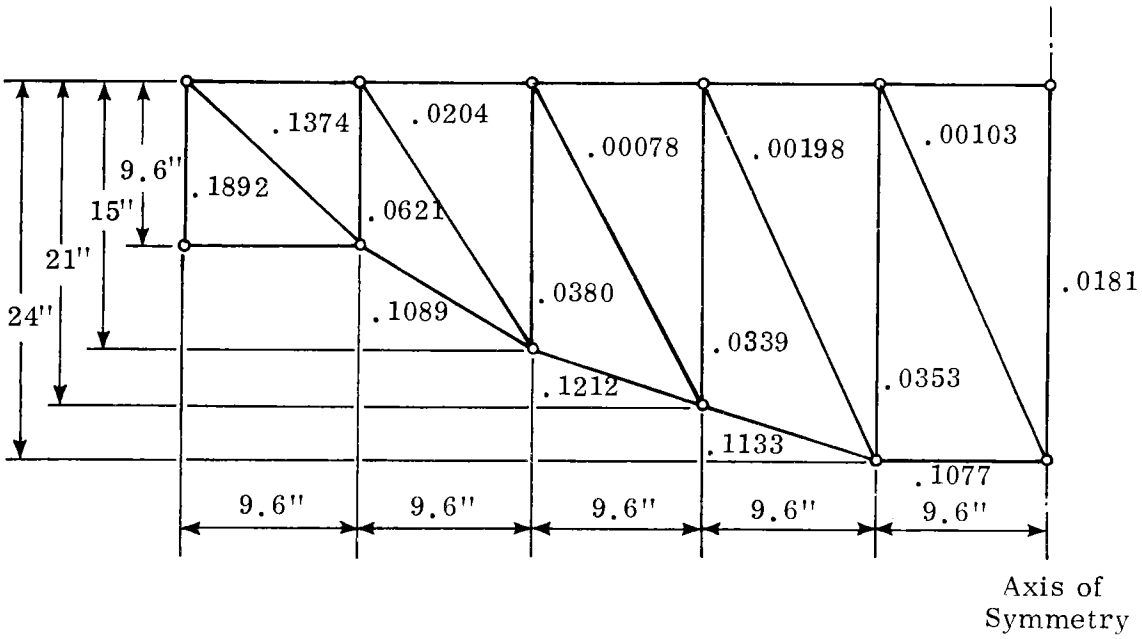

Figure 25. Intermediate shape and areas of elements of the plane truss with the 8-ft., 10-panel design. (Numbers on the elements are the areas in sq. in.)

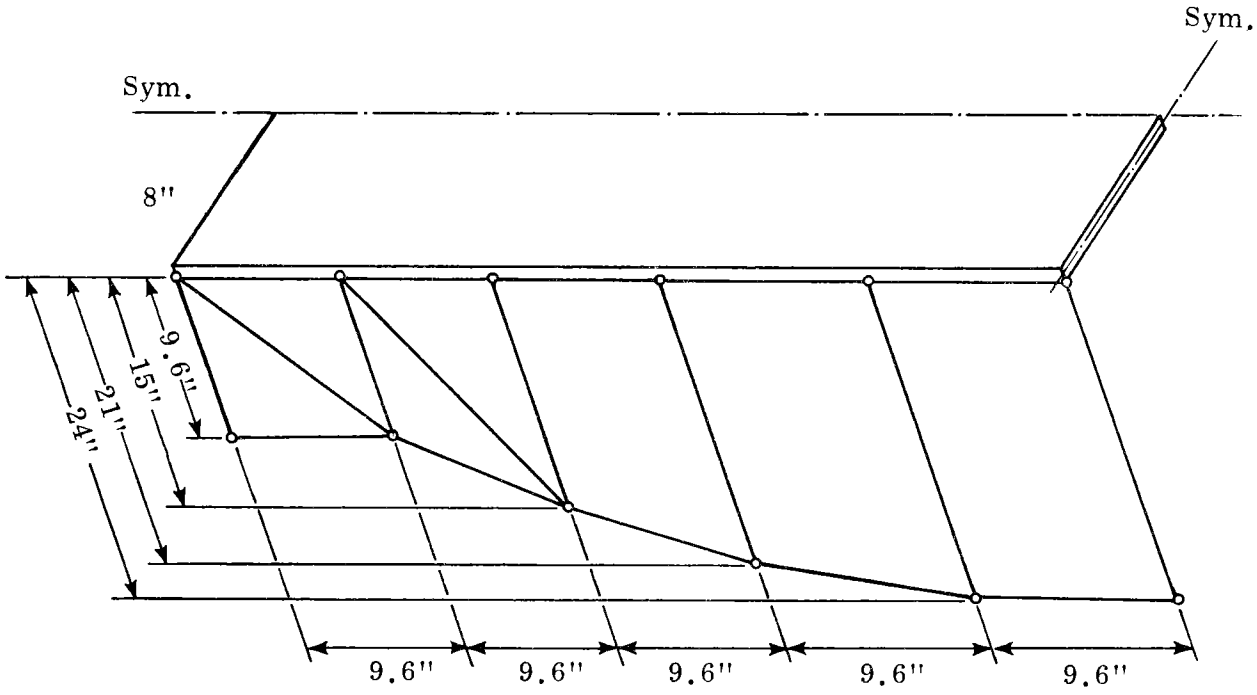

Figure 26. Final shape of the 8-ft., 10-panel design.

Table 2

Comparison of Lengths and Areas of Web and Lower Chord Elements of the Actual and Optimized Configurations of TTG-7

Element Number*	Element Length (in.)	Actual Area ($in.^2$)	Optimum Area ($in.^2$)
1	18.788	.8760	.3348
2	22.293	.0433	.2200
3	12.000	.0020	.0001
4	18.788	.4380	.3133
5	22.293	.0295	.1858
6	12.000	.0433	.1267
7	18.788	.4380	.2648
8	22.293	.0177	.1440
9	12.000	.0728	.2346
10	18.788	.4380	.2052
11	22.293	.0079	.0832
12	12.000	.0905	.3214
13	18.788	.2190	.00528

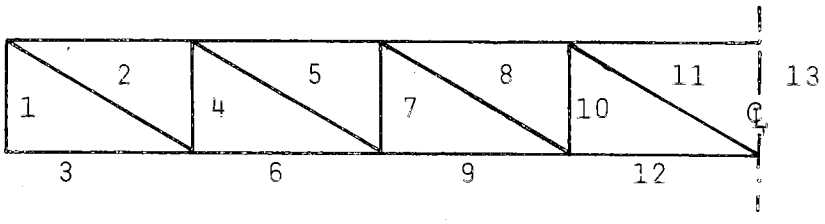

*Location of elements in TTG-7.

Table 3

Total Volumes of Web and Lower Chord Elements in the Various Designs

Member	Max. Deflection (in.)	Volume (in^3)*
Actual TTG-7 Specimen	.1717	168.66
Optimized TTG-7 Configuration	.096	166.22
8 ft. - 6 panel	.096	58.88
8 ft. - 8 panel	.096	86.42
8 ft. - 10 panel	.096	57.27
30 ft. - 8 panel	.360	3404.21
30 ft. - 10 panel	.360	4618.42

CONTACTS WITH MANUFACTURERS AND OTHERS

Some manufacturers with capabilities for fabricating triangular trussed girders were contacted. Budgetary restrictions limited visits to firms outside of the state of Virginia. Several valuable contacts were made with attendees at the Annual Meeting of the Society of Plastics Industries in February 1975 in Washington, D. C.

Other contacts of both general and specific natures were made at the following meetings:

1. ASCE/EIC/RTAC Joint Transportation Engineering Meeting, Montreal, July 1974.
2. ASCE National Structural Engineering Convention and Exposition, New Orleans, April 1975.
3. ASCE Research Council on Structural Plastics, New York, January 1975.

Technical papers describing research progress in the TTG program were presented at the first two meetings listed. A fruitful contact with the E. I. DuPont Company (manufacturer of Kevlar 49) was made at the third meeting. (A portion of the required travel funds were provided by Virginia Highway & Transportation Research Council for only the first meeting listed.) One specific conference was held with management personnel of the Baker Equipment Company of Richmond, Virginia, concerning their interest in providing fabrication services for the trussed girders. In this case, qualified interest was expressed dependent upon scheduling and volume requirements. A long established contact was maintained with a representative of the Owens Corning Fiberglas Corporation in Granville, Ohio, with the receipt of helpful advice and technical information.

Additional contacts were established with Eli Ron, Chief Engineer, Public Works Department of Tel Aviv, Israel; and Professor Y. Tene of the Israel Institute of Technology, Technion City, Haifa, Israel. Information was obtained by letter and telephone conversation with these contacts relative to the erection of a reinforced plastic pedestrian bridge in Tel Aviv in November 1972. Details related to this structure are given below.

1. Superstructure has a span of 79 feet, a width of 6 feet, and a total weight of 2.5 tons.

2. Erection time was 15 to 30 minutes at night. The superstructure may be removed intact from abutments and mounted on wheels for towing to another site.

3. No maintenance is anticipated for 20 years.

4. Entire structure was shop fabricated of an assembly of glass-reinforced plastic panels in light steel frames. Connections were made with both adhesives and welds in the steel frames. The GRP panels were hand lay-up construction.

5. A safety factor of 4 was used for the design of the GRP panels; a safety factor of 2 was used for the steel.

6. A fire-retardant polyester resin was used with additives to inhibit ultraviolet degradation. These additives increased the resin material cost by approximately 2%.

7. Initial design calculations provided for three-dimensional stress development. Laboratory tests on models were used to verify design calculations. Ultimately, a one-half scale model was load tested in a laboratory without failure. Both static and cyclic loads were applied.

8. The design live load was 93 psf.

9. The light weight of the structure does not provide sufficient damping to prevent detection of vibration by the pedestrians. The live load deflection was the limiting design factor.

10. Weathering of the resin is expected to be the primary source of deterioration of the bridge. The climatic exposure is similar to that of Florida except for lower prevailing humidities. The weathering effects are to be monitored by load testing a laboratory specimen of one-half scale after five years of exposure to the same climatic conditions as those experienced by the bridge.

11. Only one bridge was fabricated and erected due to changed economic circumstances. At the completion of the initial design, the cost of the GRP structure was 20% less than that of a reinforced concrete bridge; at the time of erection, it was 10% more. The final cost of the GRP superstructure was $12,500 and the total cost of the bridge, including design, was $45,000.

12. Other than the proposed load test of the model after five years, there is no planned program to monitor the performance of the bridge on a continuing basis.

CONCLUSIONS

The following conclusions are based on the findings of the research studies conducted.

1. Modifications to the top plate and stiffener assembly simplified the girder fabrication procedure without sacrificing load performance.

2. Load-deflection and load-strain relationships were essentially linear over the test range.

3. Use of heavier cover plates or higher modulus material for the stranded elements decreased the deformation characteristics of the member.

4. The ultimate strength of the modified style girder was in excess of a 600 psf uniformly distributed load.

5. As designed, the TTG configuration meets the requirements of span length/1000 for deflection at 85 psf as specified by AASHTO standards.

6. Maximum measured strains were relatively low (under 1/10 ultimate) for design loads of 100 psf.

7. Analytical and experimental static load test results agreed within 20% for deflections and within 30% for strains for both single and trisectional specimens. In all cases, the predicted values were higher than the experimental values.

8. The secondary creep rate was 0.03 inch per year for the centerline deflection at a load of 150 psf. Primary creep terminated after 30 days under load.

9. Elastic buckling of web elements occurred with applications of partial uniformly distributed or nonsymmetrical live loads. Analytical studies indicated that the buckling could be eliminated by providing a heavy top slab to increase the dead weight of the girder.

10. Various load tests of the trisectional specimen indicated that the principle of superposition was applicable for partial loading. It was also determined that nonsymmetrical longitudinal loading caused considerable torsional movement of the individual sections.

RECOMMENDATIONS

Laboratory Studies

Considerably more information could be obtained by continued experimentation with TTG-8 with very little cost and effort. The following steps are recommended to obtain this information.

1. Add transverse ties and struts to connect the lower chords of the sections. Conduct several load tests to compare the effects with the current structure.

2. Obtain dead weight creep data over a period of several months to compare behavior with that of TTG-6.

3. Add concrete slab and determine behavior under static load arrangements used previously.

4. Conduct cyclic load tests to study fatigue behavior.

5. Determine an ultimate static load and mode of failure.

Efforts to improve the vertical and transverse stiffener assembly should be continued. Preliminary work on a single, rigid-frame configuration to replace the four parts now used has been encouraging and should provide considerable advantages. One or more single unit test specimens similar to TTG-7 should be fabricated to verify the results of the modified stiffeners.

Additional study should be made of the use of Kevlar 49 as a substitute for glass roving. The single specimen fabricated was not representative of the best fabricating techniques nor of the geometric configuration applicable to this material. Refinements of these factors are likely to enhance the efficiency of the girder considerably.

Experimental test specimens should be studied to confirm the results of the optimization studies described earlier. These studies could be conducted jointly with the modifications to the stiffener assembly and with the use of combinations of materials.

Recommendations for a Field Installation and Study

Considerable information and knowledge has been acquired over the past several years relative to the properties of the GRP, triangular trussed girder through development studies, laboratory experiments, and industrial contacts. A full body of knowledge of this subject is certainly not complete and much more insight can be gained by further analytical and experimental work in the laboratory. At the same time, there can be no effective substitute for field studies in which all interactive variables are present, including force, temperature, moisture, sunlight, and user abuse. Therefore, it is recommended that serious thought be given to a field study of an in-service structure which would provide the opportunity for an evaluation of the behavior of the materials and performance of the overall structure under field conditions.

There are several factors which support this recommendation at this time:

1. The lead time for the verification, acceptance, and utilization of new materials and concepts is lengthy when dealing with structures involving public welfare and safety. In addition, the accumulation of much of the performance data needed for acceptance e.g., information on the environmental effects upon structural deterioration, requires long periods of time. Accelerated data collection programs, when used, have not always produced accurate predictions of time-dependent phenomena. Any anticipated adoption of new materials or untried procedures therefore should take into consideration the number of years which normally elapse between the start and finish of a developmental project.

2. Composite materials technology is continuing to develop at a rapid rate with discoveries of new products and processes. Production statistics for materials and products have increased substantially each year for the past decade (recession periods excepted) and considerable industrial expansion is now under way to meet anticipated future demand. Basic and applied research efforts continue to be strong in most areas of the reinforced plastics industry. Growing emphasis has been apparent in recent months in the area of structural applications both within and outside of the reinforced plastics industry. It is reasonable to expect that many of the technological advancements to be made in the next several years will be applicable and beneficial to highway structures. For example, there has been a recent advancement in the technology of injection molding to include chopped-glass reinforced polyester resin which portends broad replacement of structural metallic materials.(15) Cost savings of 32% have been demonstrated to date with this method of production for at least one industrial product. It is anticipated that the growth of injection molded GRP will triple in five market areas alone by 1980.

3. Public awareness of the role of synthetic materials in society is at an all time high. The use of plastic products by consumers and producers alike has reached a condition of near dependency upon these materials for convenience and potential cost reduction in almost every facet of the national lifestyle. The image of product reliability and endurance has not yet been

established for plastics as well as it has been for other more conventional materials. However, the increasing frequency of successful utilization of synthetic composites for major construction purposes should enhance the public confidence and acceptance of these materials. For example, the decision to erect the predominately plastic pedestrian bridge in Tel Aviv was an expression of confidence by Israel in an acceptable economic and functional performance of this material system.

While it would be preferable to have the bridge superstructure fabricated by a commercial firm, it is recognized that some of the unique features of the TTG member would make it difficult for a manufacturer to minimize a cost estimate for a single bridge unit. In the event that no suitable firm would be willing to undertake an experimental program of this nature, a superstructure up to 30 feet in length could be fabricated in the laboratories at the University of Virginia. Whether fabricated in-house or by a commercial firm, it is apparent that the girders would be constructed manually.

It would be essential that a location be selected for the bridge which would permit frequent visits and easy access for inspection and monitoring of applicable instrumentation. Ideally, the site should be located in the County of Albemarle, the City of Charlottesville, or perhaps on the Grounds of the University. Planning and site selection may beneficially be incorporated in the current studies for bicycle travel ways in the local community.

The proposed study for a field installation would necessarily extend over a period of time to include site selection, arrangements for substructure design and construction, superstructure fabrication, costs estimates for materials, fabrication and construction, coordination between participating organizations, and plans for monitoring the performance of the completed structure.

REFERENCES

1. McCormick, F. C., "Initial Studies of a Flexural Member Composed of Glass-Fiber Reinforced Polyester Resin," Virginia Highway & Transportation Research Council, July 1973.

2. McCormick, F. C., "Study of a Trussed Girder Composed of a Reinforced Plastic," Virginia Highway & Transportation Research Council, August 1974.

3. Michell, A. G. M., "The Limits of Economy of Material in Framed Structures," The Philosophical Magazine, S. 6, Vol. 8, No. 47, November 1904.

4. Hegemier, G. A., and W. Prager, "On Michell Trusses," International Journal of Mechanical Science, Vol. 11, 1969, pp. 209-215.

5. Prager, W., "A Note on Discretized Michell Structures," Computer Methods in Applied Mechanics and Engineering, Vol. 3, 1974, pp. 349-355.

6. Dorn, W. S., R. E. Gomory, and H. J. Greenberg, "Automatic Design of Optimal Structures," Journal de Mecanique, Paris, France, Vol. 3, No. 1, March 1964.

7. Dobbs, M. W., and L. P. Felton, "Optimization of Truss Geometry," Journal of the Structural Division, ASCE, Vol. 95, No. ST10, October 1969, pp. 2105-2118.

8. Majid, K. J., and D. W. C. Elliott, "Topological Design of Pin-Jointed Structures by Non-Linear Programming," Proceedings of the Institution of Civil Engineers, Vol. 55, Part 2, March 1973, pp. 129-149.

9. Spillers, W. R., "Iterative Design for Optimal Geometry," Journal of the Structural Division, ASCE, Vol. 101, No. ST7, July 1975, pp. 1435-1442.

10. Gellathy, R. A., and L. Berke, "Optimal Structural Design," Air Force Flight Dynamics Laboratory, AFFDL-TR-70-165, April 1971.

11. Pederson, Pauli, "On the Optimal Layout of Multi-Purpose Trusses," Computers and Structures, Vol. 2, PP. 695-712, 1972.

12. Perry, V. A. III, "Optimal Structural Design," Bachelor of Science with Honors Thesis, University of Virginia, May 1975.

13. Venkayya, V. B., "Design of Optimum Structures," Computers and Structures, Vol. 1, No. 1, August 1971, pp. 265-309.

14. Berke, L., and V. B. Venkayya, "Review of Optimality Criterial Approaches to Structural Optimization," Structural Optimization Symposium, ASME Winter Annual Meeting, November 1974, pp. 23-24.

15. Modern Plastics, August 1975, p. 16.

16. Przemieniecki, Theory of Matrix Structural Analysis, McGraw-Hill Book Company, 1968.

17. Tezcan, S., "Computer Analysis of Plane and Space Structures," ASCE, Journal of the Structural Division, April 1966, pp. 143-173.

APPENDIX A

EXPERIMENTAL TESTING

Instrumentation

Test specimens were instrumented to obtain data for vertical deflections and strains in selected elements during loading. All deflection measurements were made with conventional dial indicators with least readings of 0.001 inch. Strains were measured by means of electrical resistance strain gages bonded to the surface of the web and chord elements. Gages supplied by the Micro-Measurements Company, type EA-06-250 BF-350, were bonded with M-bond 200 adhesive to all specimens. Strains were recorded by means of a 50 channel, Model 205 indicator and Model 305 switching system made by William T. Bean, Inc.

Load Testing

All load testing was performed in the structural laboratory of the Department of Civil Engineering at the University of Virginia. Test loads were applied with hydraulic cylinders connected to a Riehle/Los pumping consele which provided load control to the nearest 20 pounds per cylinder. Air bags, 3 x 9 x 1-foot deep, made by the Uniroyal Company, were used to spread the load uniformly over the top plate of the members. Support was provided at the ends of the test member by wooden frames built to fit the triangular shape of the cross section. A 1/4-inch thick strip of elastomeric material was attached to the support frame to ensure distributed contact along the sides of the "V" of the support frame and the vertical web elements at the ends of the member. No measurements were made to determine the amount of rotation which occurred at the supports during load applications, i.e., to ascertain the degree of restraint at the support, but visual observations of the member indicated that no obvious end restraint was present. No effort was made to control the environmental conditions of the laboratory during the period of load testing. In general, the temperature ranged from 68°F to 75°F and the relative humidity from 45% to 65%.

STRESS ANALYSIS AND DESCRIPTION OF COMPUTER PROGRAM

Axial stresses in the web and lower chord elements and displacements at the joints were computed theoretically by the finite element method utilizing plate bending elements to represent the top plate and space truss elements for the web and lower chord. The relationship between the forces and displacements at the nodes of an element is

$$q_i = \sum_{j=1}^{n} k_{ij} d_j$$

where q_i is a force in direction i; the stiffness coefficient, k_{ij}, is the force that must be applied in direction i to produce a unit deformation in direction j when no other deformations occur in the element; and d_j is the deformation in direction j. Expressed in matrix notation, the relation becomes

$$\{q\} = [k]\ \{d\}$$

The stiffness matrix [k]of a space truss element, with reference to the global coordinates as shown in Figure A-1, is

$$[k] = \frac{AE}{L} \begin{bmatrix} l^2 & & & & & \\ lm & m^2 & & \text{symmetric} & & \\ ln & mn & n^2 & & & \\ -l^2 & -lm & -ln & l^2 & & \\ -lm & -m^2 & -mn & lm & m^2 & \\ -ln & -mn & -n^2 & ln & mn & n^2 \end{bmatrix}$$

where $l = \frac{X_b - X_a}{L}$, $m = \frac{Y_b - Y_a}{L}$, $n = \frac{Z_b - A_a}{L}$

The stiffness matrix for the rectangular plate bending element shown in Figure A-2 was taken from Przemieniecki.[16] It was derived using a displacement function that ensures both deflection and slope compatibility on adjacent elements.

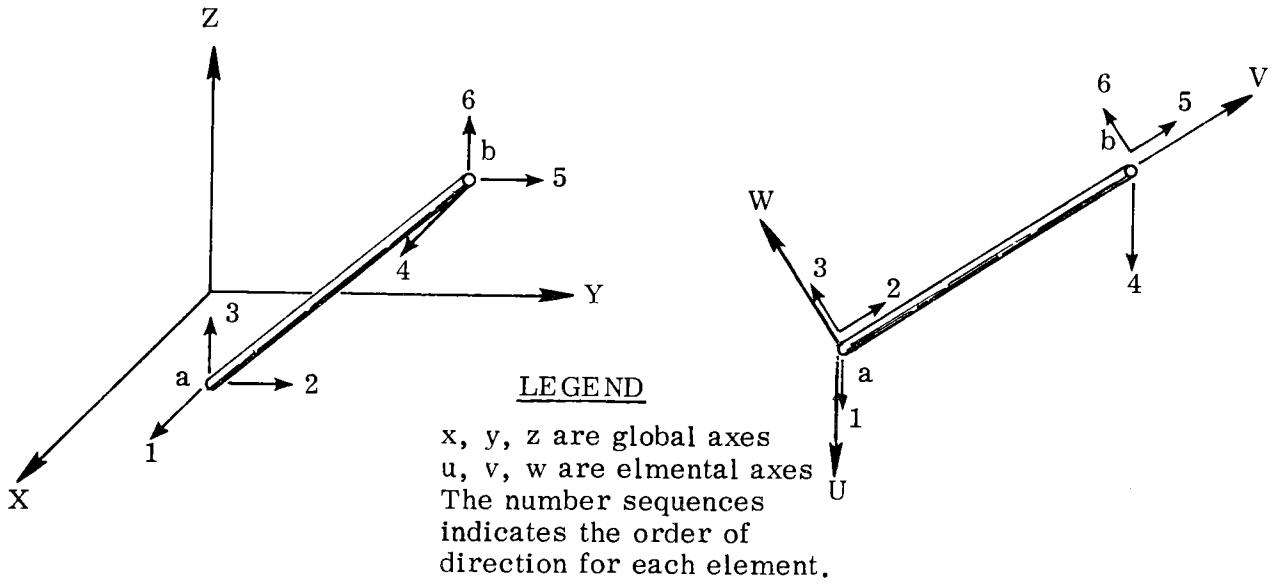

Figure A-1. Global and element axes for space truss element.

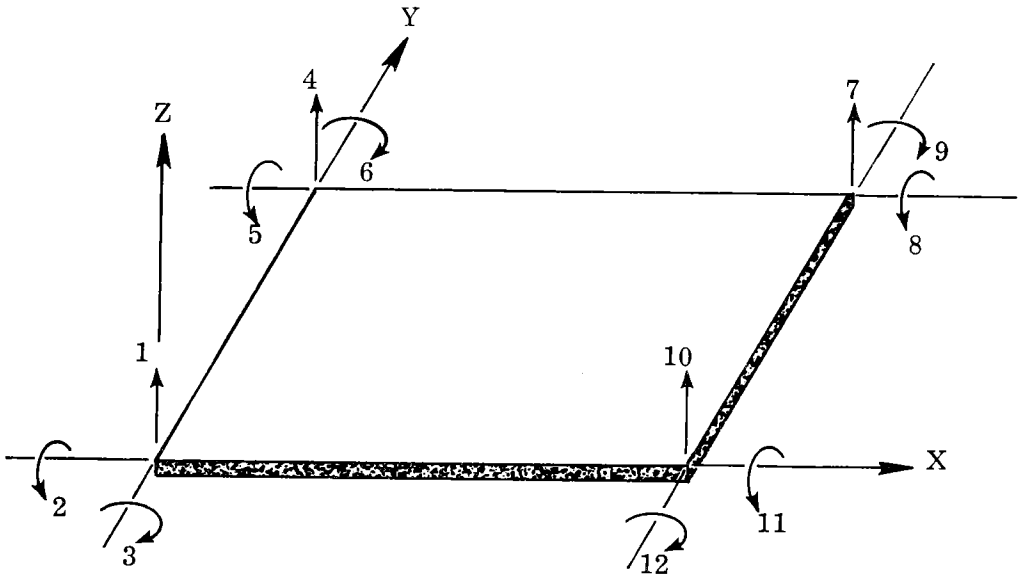

Figure A-2. Rectangular plate bending element.

The stiffness matrix [K] for the entire structure (one or more girder sections) is generated by superposition of the matrices of each element. If the external forces and corresponding displacements of the joints in the truss are denoted by {Q} and {D} respectively, the matrix equation for the load-displacement respectively, the matrix equation for the load-displacement relationship of the entire structure may be shown as

$$\{Q\} = [K] \{D\}$$

Figure A-3 shows schematically the set of directions by which the forces and displacements were defined. Two planes of symmetry permitted use of only one-quarter of the structure in the analyses, and thereby reduced the number of the numerical calculations. For a given load vector {Q}, this set of linear simultaneous equations may be solved for {D}. Thereafter, the deformation vector (d_{xyz}) of each element can be obtained. Subsequent multiplication of $\{d_{xyz}\}$ by $\{k_{xyz}\}$ gives values for $\{q_{xyz}\}$ as desired. The final axial force in each bar is obtained by transforming the xyz components into the element axes (or uvw direction) by

$$\{q\} = [T] \{q\}_{xyz}$$

where [T] is a transformation matrix as defined below:

$$[T] = \begin{bmatrix} [t] & & \\ & & \\ & & [t] \end{bmatrix}$$

$$[t] = \begin{bmatrix} \frac{m}{Q} & \frac{-l}{Q} & 0 \\ l & m & n \\ \frac{-ln}{Q} & \frac{-mn}{Q} & Q \end{bmatrix}$$

$$Q = \left|\sqrt{1 - n^2}\right|$$

For vertical bars, Q is zero because $n = \pm 1$, and some quantities in [t] become indefinite. Therefore, for vertical bars

$$[t] = \begin{bmatrix} 0 & -1 & 0 \\ 0 & 0 & n \\ -n & 0 & 0 \end{bmatrix}$$

(Reference 17)

Final values are presented in unit stresses and strains.

Final computations are printed as axial stress and strain for each element and the deflections of each panel point. A complete listing of the computer program is included in the following pages.

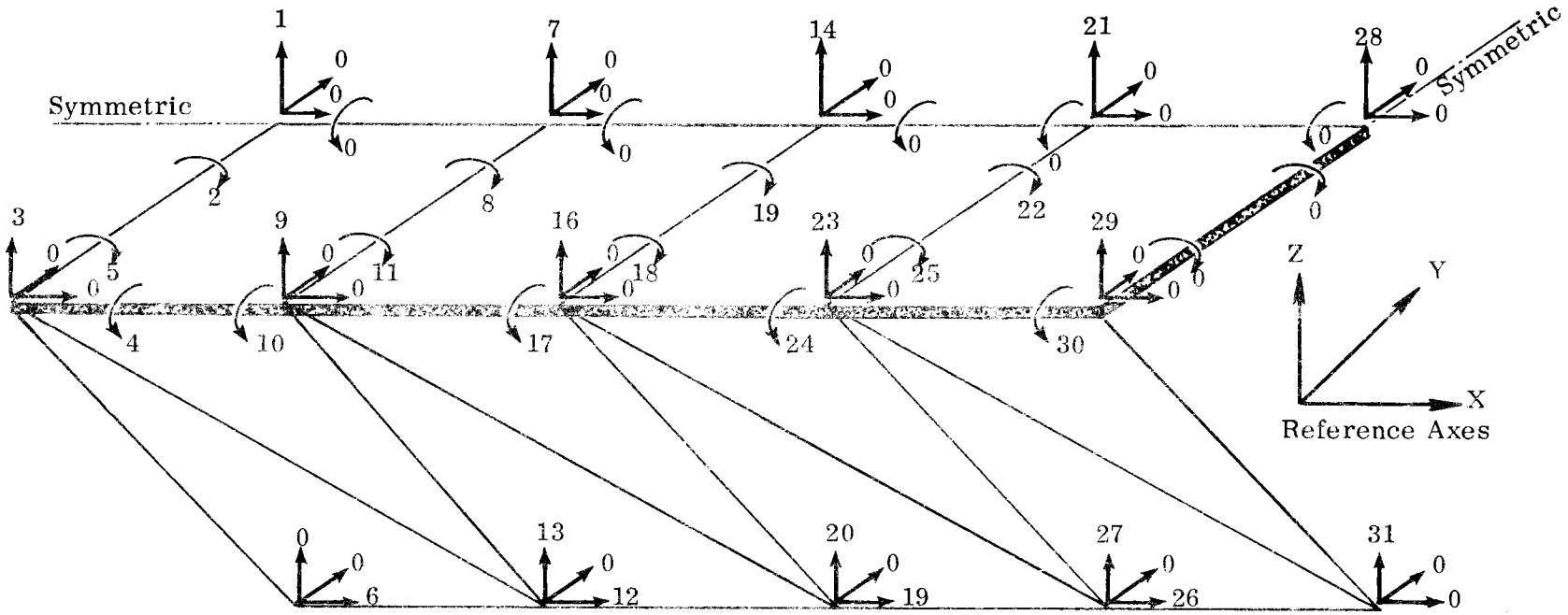

Figure A-3. Displacement directions of a one-section structure with two planes of symmetry. (The numbers refer to independent possible motions.)

```
      PROGRAM FIG(INPUT,OUTPUT,TAPE5=INPUT,TAPE6=OUTPUT,TAPE1)
C     ******************************************************************
C     FINITE ELEMENT ANALYSIS OF 3 DIMENSIONAL STRUCTURES CONSISTING OF
C     PLATE BENDING AND SPACE TRUSS ELEMENTS.
C     STIFFNESS MATRIX FOR A RECTANGULAR PLATE ELEMENT IS TAKEN FROM
C     PRZEMIENIECKI,S THEORY OF MATRIX STRUCTURAL ANALYSIS.
C
C     H.ALPER,  MARCH 1975
C     ******************************************************************
000003      DIMENSION TITLE(20),S(75,75),P(75),NCODE(65,12),BSM(6,6),DM(12)
000003      DIMENSION D(75) ,PSM(12,12),EY(3),PR(3),PM(6),PMI(6),T(6,6)
000003      DIMENSION ITYPE(65),LOIR(75),TEMP(75)
000003      DIMENSION ST(3,12),XMOM(3)
000003      IFLAG=0
C     NPROB=NO. OF PROBLEM
000004  999 READ(5,1) NPROB,(TITLE(J),J=1,19)
000020    1 FORMAT(I4,19A4)
000020      IF(NPROB.LE.0) GO TO 9999
000022      WRITE(6,2)(TITLE(J),J=1,19)
000033    2 FORMAT(1H1,///24X,20A4)
C     ME=NO. OF MEMBERS, N=NO. OF DEGREES OF FREEDOM
C     NMAT=NO. OF DIFFERENT MATERIALS
000033      READ(5,29) ME,N,NMAT,NLOAD
C     READ AND PRINT MODULUS OF ELASTICITY AND POISSON RATIO FOR EACH MATERIAL
000047      WRITE(6,16)
000053   16 FORMAT(//30X,12HMATERIAL NO.,6X,12HMOD.OF ELAS.,6X,13HPOISSON RATI
     1O)
000053      READ(5,17)(EY(I),PR(I),I=1,NMAT)
000070   17 FORMAT(2F10.0)
000070      WRITE(6,18)(I,EY(I),PR(I),I=1,NMAT)
000106   18 FORMAT(35X,I3,6X,E15.6,3X,E15.6)
000106   41 FORMAT(6F10.0)
000106      DO 15 I=1,N
000110      DO 15 J=1,N
000111   15 S(I,J)=0.
000120      WRITE(6,19)
000123   19 FORMAT(///1X,7HELEMENT,1X,4HMTRL,4X,8HX COMP/A,5X,8HY COMP/B,5X,16
     1HZ COMP/THICKNESS,5X,4HAREA,5X,12HCODE NUMBERS)
000123      MTAPE=1
000124      REWIND MTAPE
000126      DO 20 M=1,ME
000130      READ(5,33)ITYPE(M),MAT,X,Y,Z,A
000147   33 FORMAT(2I5,4F10.0)
C     ITYPE=1 FOR PLATE BENDING ELEMENTS, 2 FOR TRUSS ELEMENTS
C     MAT=WHICH MATERIAL IS THE ELEMENT MADE OF
C     X=LENGTH OF PLATE IN X-DIR. OR X(J)-X(I) OF BAR
C     Y=LENGTH OF PLATE IN Y-DIR. OR Y(J)-Y(I) OF BAR
C     Z=THICKNESS OF PLATE OR Z(J)-Z(I) OF BAR
C     A=AREA OF BAR
000147      PO=PR(MAT)
000151      E=EY(MAT)
000153      READ(5,29)(NCODE(M,J),J=1,12)
000166   29 FORMAT(12I5)
000166      IF(ITYPE(M).EQ.1) GO TO 27
000171      DL=(X**2+Y**2+Z**2)**.5
000177      CL=X/DL
000201      EP=1/DL
```

```
000202          EN=Z/DL
000204          CALL BARST(E,A,DL,EL,EM,EN,BSM)
000212          WRITE(9TAPE)BSM,EL,EM,EN,A,E
000231          KODE=6
000232          GO TO 28
000233       27 CALL PLST(E,PO,X,Y,Z,PSM)
000237          WRITE(9TAPE) E,PO,X,Y,Z
000254          KODE=12
000255       28 WRITE(6,34)M,MAT,X,Y,Z,A,(NCODE(M,J),J=1,KODE)
000306       34 FORMAT(2X,I3,3X,I3,3F14.3,F14.5,12I5)
000306          DO 35 I=1,KODE
000310          IF(NCODE(M,I).EQ.0) GO TO 35
000313          K=NCODE(M,I)
000316          DO 45 J=1,KODE
000320          IF(NCODE(M,J).EQ.0) GO TO 45
000323          L=NCODE(M,J)
000326          IF(ITYPE(M).EQ.1) GO TO 651
000330          S(K,L)=S(K,L)+BSM(I,J)
000337          GO TO 45
000340      651 S(K,L)=S(K,L)+PSM(I,J)
000347       45 CONTINUE
000352       35 CONTINUE
000355       20 CONTINUE
              C     SYSTEM STIFFNESS MATRIX GENERATED
000357          LCON=0
000360      888 LCON=LCON+1
000362          IF(LCON.GT.NLOAD) GO TO 999
000365          DO 710 J=1,N
000366      710 P(J)=0.
000371          READ(5,29) NLDIR
000377          READ(5,29) (LDIR(I),I=1,NLDIR)
000412          READ(5,10) (TEMP(I),I=1,NLDIR)
000425       10 FORMAT(8F10.0)
000425          DO 725 I=1,NLDIR
000427          J=LDIR(I)
000431      725 P(J)=TEMP(I)
000435          WRITE(6,55) LCON
000442       55 FORMAT(///40X,14HLOAD CONDITION,I3)
000442          DO 60 J=1,N
000444       60 WRITE(6,65)J,P(J)
000456       65 FORMAT(40X,2HP(,I2,2H)=,F13.5)
000456          WRITE(6,68)
000461       68 FORMAT(///40X,18HJOINT DEFORMATIONS)
              C     THE MATRIX EQUATION KD=P IS SOLVED BY GAUSSIAN ELIMINATION METHOD
000461          CALL GAUSS(S,D,P,N,IFLAG)
000465          IF(IFLAG.EQ.1) GO TO 999
000470          DO 80 I=1,N
000471       80 WRITE(6,85) I,D(I)
000503       85 FORMAT(40X,2HD(,I2,2H)=,F10.7)
000503          WRITE(6,90)
000506       90 FORMAT(///14X,6HMEMBR NO.,5X,13HBAR AX. FORCE,5X,6HSTRESS,10X,6HSTR
             1AIN,15X,24HX,14X,2HY,11X,3HMXY//)
              C     FOR EACH BAR THE DISPLACEMENT MATRIX IS DETERMINED UTILIZING CODE
              C     NUMBERS AND MEMBER END FORCES ARE FOUND BY PREMULTIPLYING BY THE
              C     MEMBER STIFFNESS MATRICES.
000506          REWIND 9TAPE
000510          DO 120 M=1,MM
000512          IF(ITYPE(M).EQ.1) GO TO 125
```

```
000514          READ(MTAPE)BSM,EL,EM,EN,A,E
000533          DO 130 I=1,6
000535          DM(I)=0.
000536          PM(I)=0.
000537          K=NCODE(M,I)
000543          IF(K.EQ.0) GO TO 130
000544          DM(I)=D(K)
000545      130 CONTINUE
000547          DO 140 I=1,6
000551          DO 140 J=1,6
000552      140 PM(I)=PM(I)+BSM(I,J)*DM(J)
000564          DO 502 I=1,6
000565      502 PMI(I)=0.
000570          CALL TRANS(EL,EM,EN,T)
000573          DO 445 I=1,6
000575          DO 445 J=1,6
000576      445 PMI(I)=PMI(I)+T(I,J)*PM(J)
000610          IF(A.LT.1.E-8)  GO TO 120
000612          SIG=PMI(5)/A
000614          EPS=SIG/E
000616          WRITE(6,875)M,PMI(5),SIG,EPS
000631      875 FORMAT(17X,I3, 8X,3E15.6)
000631          GO TO 120
000632      125 READ(MTAPE) E,PO,X,Y,Z
000647          DO 158 I=1,12
000651          DM(I)=0.
000652          K=NCODE(M,I)
000656          IF(K.EQ.0) GO TO 158
000657          DM(I)=D(K)
000660      158 CONTINUE
            C       MOMENTS AT CENTER OF PLATE ARE CALCULATED
000662          X2=X/2.
000664          Y2=Y/2.
000666          CALL STRESS(E,PO,X,Y,Z,ST,X2,Y2)
000675          DO 150 I=1,3
000677          XMOM(I)=0.
000700          DO 160 J=1,12
000702      160 XMOM(I)=XMOM(I)+ST(I,J)*DM(J)
000711      150 CONTINUE
000713          WRITE(6,200) M,  (XMOM(I),I=1,3)
000727      200 FORMAT(17X,I3,55X,3E15.6)
000727      120 CONTINUE
000732          GO TO 100
000732     9999 STOP
000734          END
```

1272

```
      SUBROUTINE ASSTIF(A,JLAEL,EM,ELEN,NSM)
C     SPACE TRUSS MEMBER STIFFNESS MATRIX
      REAL L,M,N
      DIMENSION A(6,6)
      L=EL
      M=EM
      N=EN
      S=AE/EL
      A(1,1)=L*L
      A(2,1)=L*M
      A(3,1)=L*N
      A(4,1)=-L*L
      A(5,1)=-L*M
      A(6,1)=-L*N
      A(2,2)=M*M
      A(3,2)=M*N
      A(4,2)=-L*M
      A(5,2)=-M*M
      A(6,2)=-M*N
      A(3,3)=N*N
      A(4,3)=-L*N
      A(5,3)=-M*N
      A(6,3)=-N*N
      A(4,4)=L*L
      A(5,4)=L*M
      A(6,4)=L*N
      A(5,5)=M*M
      A(6,5)=M*N
      A(6,6)=N*N
      DO 5 I=1,6
      DO 5 J=1,6
    5 A(I,J)=S*A(I,J)
      DO 6 I=1,6
      DO 6 J=1,6
    6 A(I,J)=A(I,J)*NSM
      RETURN
      END
```

```
      SUBROUTINE PLST(E,PO,A,F,T,S)
C     RECTANGULAR PLATE BENDING ELEMENT STIFFNESS MATRIX
      DIMENSION S(12,12)
      C=E/A
      U=C*C
      V=1./U
      D=E*T**3/(12.*(1.-PO*PO))*A*U
      S(1,1)=156.*(U+V)/35.+72./25.
      S(2,1)=F*(22.*U/35.+7.*(35.*U)+6.*(1.+5.*PO)/25.)
      S(3,1)=-A*(22.*U/35.+22./(35.*U)+6.*(1.+5.*PO)/25.)
      S(4,1)=54.*U/35.-156./(35.*U)-72./25.
      S(5,1)=F*(-13.*U/35.+7.*V/35.+6./25.)
      S(6,1)=A*(-22.*U/35.+22.*V/35.+6.*(1.+5.*PO)/25.)
      S(7,1)=-54.*(U+V)/35.+72./25.
      S(8,1)=F*(13.*U/35.+27.*V/35.-6./25.)
      S(9,1)=F*(-27.*U/35.-13.*V/35.+6./25.
      S(10,1)=-156.*U/35.+54.*V/35.-72./25.
      S(11,1)=F*(-27.*U/35.+27.*V/35.-6.*(1.+5.*PO)/25.)
      S(12,1)=F*(-13.*U/35.+13.*V/35.-6./25.)
      S(2,2)=F*U*(4.*U/35.+52.*V/35.+8./25.)
      S(3,2)=-A*(11.*(U+V)/35.+(1.+66.*PO)/50.)
      S(4,2)=F*(13.*U/35.-78.*V/35.-6./25.)
      S(5,2)=F*(-3.*U/35.+26.*V/35.-0.04)
      S(6,2)=A*(-13.*U/70.+11.*V/35.+(1.+5.*PO)/50.)
      S(7,2)=F*(-13.*U/35.-27.*V/35.+6./25.)
      S(8,2)=F*(3.*U/35.+9.*V/35.+2./25.)
      S(9,2)=A*(-13.*(U+V)/70.+1./50.)
      S(10,2)=F*(-22.*U/35.+27.*V/35.-6.*(1.+5.*PO)/25.)
      S(11,2)=A*(-4.*U/35.+10.*V/35.-6./25.)
      S(12,2)=A*(-11.*U/35.+13.*V/70.-(1.+5.*PO)/50.)
      S(3,3)=A*(52.*U/35.+4.*V/35.+8./25.)
      S(4,3)=A*(-22.*U/35.+22.*V/35.+6.*(1.+5.*PO)/25.)
      S(5,3)=A*(17.*U/70.-11.*V/35.-(1.+5.*PO)/50.)
      S(6,3)=A*(10.*U/35.-4.*V/35.-8./25.)
      S(7,3)=F*(27.*U/35.+13.*V/35.-6./25.)
      S(8,3)=A*(11.*(U+V)/70.-3.02)
      S(9,3)=A*(6.*U/35.+3.*V/35.+2./25.)
      S(10,3)=A*(17.*U/35.-13.*V/35.+6./25.)
      S(11,3)=A*(11.*U/35.-13.*V/70.+(1.+5.*PO)/50.)
      S(12,3)=A*(26.*U/35.-3.*V/35.-2./25.)
      S(4,4)=S(1,1)
      S(5,4)=S(2,1)
      S(6,4)=S(3,1)
      S(7,4)=S(10,1)
      S(8,4)=S(11,1)
      S(9,4)=S(12,1)
      S(10,4)=S(7,1)
      S(11,4)=S(8,1)
      S(12,4)=S(9,1)
      S(5,5)=S(1,1)
      S(6,5)=S(2,1)
      S(7,5)=S(4,1)
      S(8,5)=S(5,1)
      S(9,5)=S(6,1)
      S(10,5)=S(10,2)
      S(11,5)=S(11,2)
      S(12,5)=S(12,2)
      S(6,6)=S(1,1)
      S(7,6)=S(4,2)
      S(8,6)=S(5,2)
      S(9,6)=S(6,2)
      S(10,6)=S(10,3)
      S(11,6)=S(11,3)
      S(12,6)=S(12,3)
      S(7,7)=S(1,1)
      S(8,7)=S(2,1)
      S(9,7)=S(3,1)
      S(10,7)=S(10,4)
      S(11,7)=S(11,4)
      S(12,7)=S(12,4)
      S(8,8)=S(1,1)
      S(9,8)=S(3,2)
      S(10,8)=S(10,5)
      S(11,8)=S(11,5)
      S(12,8)=S(12,5)
      S(9,9)=S(1,1)
      S(10,9)=S(4,3)
      S(11,9)=S(5,3)
      S(12,9)=S(6,3)
      S(10,10)=S(1,1)
      S(11,10)=S(2,1)
      S(12,10)=S(3,1)
      S(11,11)=S(1,1)
      S(12,11)=S(2,1)
      S(12,12)=S(1,1)
      RETURN
      END
```

```
000463          S(7,7)=S(3,3)
000464          S(7,8)=S(10,3)
000465          S(8,8)=-S(11,3)
000467          S(9,8)=S(12,3)
000471          S(10,8)=S(7,3)
000472          S(11,8)=S(8,3)
000474          S(12,8)=S(9,3)
000475          S(7,7)=S(1,1)
000477          S(8,7)=-S(2,1)
000500          S(9,7)=-S(3,1)
000502          S(10,7)=S(4,1)
000503          S(11,7)=-S(5,1)
000505          S(12,7)=-S(6,1)
000506          S(8,8)=S(2,2)
000510          S(9,8)=S(3,2)
000511          S(10,8)=-S(4,2)
000513          S(11,8)=S(5,2)
000514          S(12,8)=S(6,2)
000516          S(9,9)=S(3,3)
000517          S(10,9)=-S(4,3)
000521          S(11,9)=S(5,3)
000522          S(12,9)=S(6,3)
000524          S(10,10)=S(4,4)
000525          S(11,10)=-S(5,4)
000527          S(12,10)=-S(6,4)
000530          S(11,11)=S(5,5)
000532          S(12,11)=S(6,5)
000533          S(12,12)=S(6,6)
000535          DO 5 I=1,12
000536          DO 5 J=I,12
000537        5 S(I,J)=S(J,I)
000551          DO 8 I=1,12
000552          DO 8 J=1,12
000553        8 S(I,J)=D*S(I,J)
000563          RETURN
000564          END
```

```
                SUBROUTINE TRANS(EL,EM,EN,T)
          C     TRANSFORMATION MATRIX FOR A SPACE TRUSS ELEMENT
000007          REAL L,M,N
000007          DIMENSION T(6,6)
000007          L=EL
000010          M=EM
000011          N=EN
000012          DO 5 I=1,6
000013          DO 5 J=1,6
000014        5 T(I,J)=0.
000023          IF(ABS(N-1.).LE.1.E-8.OR.ABS(N+1.).LE.1.E-8) GO TO 15
000042          Q=ABS(SQRT(1.-N*N))
000050          T(1,1)=M/Q
000054          T(1,2)=-L/Q
000056          T(2,1)=L
000057          T(2,2)=M
000060          T(2,3)=N
000062          T(3,1)=-L*N/Q
000064          T(3,2)=-M*N/Q
000066          T(3,3)=Q
000067          T(4,4)=M/Q
000070          T(4,5)=-L/Q
000072          T(5,4)=L
000073          T(5,5)=M
000074          T(5,6)=N
000076          T(6,4)=-L*N/Q
000100          T(6,5)=-M*N/Q
000102          T(6,6)=Q
000103          GO TO 25
000104       15 T(1,2)=-1.
000106          T(2,3)=N
000107          T(3,1)=-N
000110          T(4,5)=-1.
000111          T(5,6)=0
000112          T(6,4)=-N
000113       25 CONTINUE
000113          RETURN
000114          END
```

```
      SUBROUTINE GAUSS(A,X,BH,N,IFLAG)
000010      DIMENSION S(75,77),R(75),A(75,75),W(75,77),B(75),X(75)
000010      DIMENSION J(75),P(75),D(75)
C  SOLUTION OF AX=P BY GAUSSIAN ELIMINATION
000010      DET=1.
000011      NP1=N+1
000013      NP2=N+2
000015      NM1=N-1
C  FORM VECTORS D AND P
000016      DO 2 I=1,N
000017      P(I)=I
000021      D(I)=ABS(A(I,1))
000023      DO 2 J=2,N
000025      IF(D(I).LT.ABS(A(I,J)))    D(I)=ABS(A(I,J))
000041    2 CONTINUE
C  ESTABLISH WORKING MATRIX W
000046      DO 3 I=1,N
000047      DO 3 J=1,N
000050    3 W(I,J)=A(I,J)
000061      DO 4 I=1,N
000062      W(I,NP1)=B(I)
000066    4 W(I,NP2)=P(I)
C  TAKE A COLUMN TO START ELIMINATION
000073      DO 5 J=1,NM1
CALCULATE AND COMPARE Q*S
000074      QMAX=0.
000075      DO10 I=J,N
000076      Q(I)=ABS(W(I,J))/W(I,NP1)
000105      IF(Q(I)-QMAX) 10,10,8
000110    8 QMAX=Q(I)
000112      M=I
000113   10 CONTINUE
C  EXCHANGE ROWS IF NECESSARY
000116      IF(M.EQ.J) GO TO 20
000120      DET=-DET
000121      DO 15 JJ=1,NP2
000122      S(J,JJ)=W(J,JJ)
000127      W(J,JJ)=W(M,JJ)
000132   15 W(M,JJ)=S(J,JJ)
C  TAKE A ROW, CALCULATE R(I,J), STORE IN W(I,J)
000137   20 JP1=J+1
000141      DET=DET*W(J,J)
000145      DO 5 I=JP1,N
000147      W(I,J)=W(I,J)/W(J,J)
C  ELIMINATION
000154      DO 5 K=JP1,N
000156      W(I,K)=W(I,K)-W(I,J)*W(J,K)
000170    5 CONTINUE
000176      DET=DET*W(J,J)
000201      IF(ABS(DET).LT.1.E-10)   GO TO 705
000204      DO 25 I=1,N
000206      I P2=W(I,NP2)
000212   25 B(I)=W(I,NP2)
C  MODIFY B VECTOR
000216      DO 56 J=1,NM1
000220      JP1=J+1
000222      DO 56 I=JP1,N
```

```
000224      SUBROUTINE P(I)=A(I,J)*B(J)
            C  MAGP SUBSTITUTE
000236            X(I)=B(I)/W(I,I)
000244            DO 101 K=2,N
000245            J=I-K+1
000247            SUM=0.
000250            JJ=J+1
000252            DO 115 I=JJ,I
000253      115   SUM=SUM+A(J,I)*X(I)
000263      101   X(J)=(B(J)-SUM)/W(J,J)
000274            RETURN
000274      705   UPLIE(6,730)
000300      730   FORMAT(//20X,35HSYSTEM STIFFNESS MATRIX IS SINGULAR)
000300            IFLAG=1
000304            RETURN
000305            END
```

APPENDIX B

THEORY OF OPTIMALITY CRITERIA FOR STRUCTURAL DESIGN
(This section is taken from Reference 12 with some modifications.)

The application of optimality criteria approaches to structural optimization involves deriving optimality criteria for the specified design conditions and establishing an iterative procedure for achieving the optimum design. In contrast to mathematical programming methods, a characterization of the optimal state of the structure is provided, but no preferred path for reaching that state is given. Direct intuitive procedures are used for the structural resizing necessary to achieve the optimal design. Such approaches usually involve simple recursion relations which are very efficient and easily programmed for the computer.

Derivations of the Optimality Criterion

The objective is to minimize the weight of the structure while satisfying the desired stiffness characteristics under specified loading conditions. The configuration of the structure is assumed to be fixed and the total structure is discretized into infinite elements. For a truss the only design variables are the areas of the elements. Under these conditions the total weight of the structure may be expressed as

$$W = \sum_{i=1}^{m} \rho_i A_i \ell_i \qquad \text{(A-1)}$$

where ρ_i is the mass density, A_i is the area, and ℓ_i is the length of i^{th} element.

By the principle of minimum potential energy, the structure is in equilibrium when

$$(U + V) = 0 \qquad \text{(A-2)}$$

where

$$U = \tfrac{1}{2} \{r\}^t [K] \{r\} \qquad \text{(A-3)}$$

is the total strain energy of the structure, and

$$V = - \{R\}^t \{r\} \qquad \text{(A-4)}$$

is the potential energy of applied loads. Then the equilibrium constraint is

$$\delta \left[\tfrac{1}{2} \{r\}^t [K] \{r\} - \{R\}^t \{r\}\right] = 0 \qquad \text{(A-5)}$$

where [K] is the structure stiffness matrix, {R} is the vector of applied loads, and {r} is the structure displacement vector.

Constraints on minimum element areas can be expressed as

$$A_i \geq a_i \qquad \text{(A-6)}$$

where a_i is a constant. This equality can be converted into an equality constraint by introducing a vector of slack variables x_i:

$$A_i - a_i - x_i^2 = 0 \qquad \text{(A-7)}$$

Stress constraints can be imposed as

$$\sigma_i \leq \sigma_{max} \qquad \text{(A-8)}$$

where σ_i is the effective stress in the element and σ_{max} is the maximum allowable stress. For a truss the effective stress would be the axial stress in the element. Introducing another vector of slack variables y_i, the stress constraints can be expressed as

$$\sigma_i - \sigma_{max} - y_i^2 = 0 \qquad \text{(A-9)}$$

The optimization problem can now be written as finding the minimum value of

$$W(A) = \sum_{i=1}^{m} \rho A_i \ell_i \qquad \text{(A-10)}$$

subject to the constraints

$$\tfrac{1}{2} \{r\}^t [K] \{r\} - \{R\}^t \{r\} = 0$$

$$\{A\} - \{a\} - \{x^2\} = 0$$

$$\{\sigma\} - \sigma_{max} - \{y_i^2\} = 0 \qquad \text{(A-11)}$$

According to the theory of the calculus of several variables, when the equality constraint equations are added to the objective functions using Lagrange multipliers, the problem reduces to finding the stationary value of the functional ϕ such that

$$\phi = \sum_{i=1}^{m} \rho A_i \ell_i - \lambda_1 [\tfrac{1}{2} \{r\}^t [K] \{r\} - \{R\}^t \{r\} - \lambda_2 [\{A\} - \{a\} - \{x^2\} - \lambda_3 [\{\sigma\} - \sigma_{max} - y^2 \quad \text{(A-12)}$$

Here ϕ is a function of the nodal displacements $\{r\}$ the design variables $\{A\}$, the slack variables $\{x^2\}$ and $\{y^2\}$ and the Lagrange multipliers λ_1, λ_2, and λ_3. To determine the stationary value of the functional ϕ, the variations with respect to the above variables should be obtained and set equal to zero. The variation of ϕ with respect to the displacements gives

$$\phi_r = \lambda_1 \left[[K] \{r\} - \{R\} \right] = 0 \quad \text{(A-13)}$$

which is the equilibrium equation of the structure. The variation of ϕ with respect to the slack variables gives

$$\phi_x = 2 \lambda_2 \{x\} = 0 \quad \text{(A-14)}$$

$$\phi_y = 2 \lambda_3 \{y\} = 0 \quad \text{(A-15)}$$

When either the stress or the minimum area constraints for an element are active, no further reduction in its area can occur, so the slack variable for these constraints are zero. However, when neither constraint is active, further modification in its area is possible, and slack variables are not zero. Therefore, from equations A-14 and A-15 the Lagrange multipliers associated with them must vanish. Thus equation A-12 reduces to

$$\phi^1 = \sum_{i=1}^{m} \rho A_i \ell_i - \lambda_1 \left[\tfrac{1}{2} \{r\}^t [K] \{r\} - \{R\}^t \{r\} \right] \quad \text{(A-16)}$$

The variation of ϕ^1 with respect to the design variables gives

$$\phi^1_{A_i} = \rho \ell_i - \lambda_1 \left[\tfrac{1}{2} \{r\}^t \frac{\partial K}{\partial A_i} \{r\} \right] = 0 \qquad \text{(A-17)}$$

The stiffness matrix of the structure can be expressed as the sum of the stiffness matrices of its elements as

$$[K] = \sum_{i=1}^{m} [K_i] \qquad \text{(A-18)}$$

where K_i is the stiffness matrix of i^{th} element in global coordinates. Since only the stiffness matrix of i^{th} element is affected by a change in A_i

$$\frac{\partial [K]}{\partial A_i} = \frac{\partial [K_i]}{\partial A_i} \qquad \text{(A-19)}$$

and for a truss

$$\frac{\partial [K_i]}{\partial A_i} = \frac{1}{A_i} [K_i] \qquad \text{(A-20)}$$

Substituting equation A-20 into equation A-17 gives

$$\frac{\tfrac{1}{2} \{r\}^t [K_i] \{r_i\}}{\ell_i A_i} = \frac{\rho}{\lambda_1} = \delta = \text{constant} \qquad \text{(A-21)}$$

The statement of the optimality criterion follows from equation A-21: the optimal structure is one in which the strain energy density is the same in all its elements that are not affected by the stress or minimum area constraints.

Venkayya[13,14] points out that for statically determinate structures this optimality criterion is a necessary and sufficient condition for global optimality. However in the case of statically indeterminate structures, it is usually possible to find more than one design which satisfies the optimality criterion. Each of these designs represents a relative minimum.

Formulation of the Optimization Algorithm

The next step is the development of a numerical procedure for arriving at a design which satisfies the optimality criterion.

Assume that there is a design vector {A} in the feasible domain. This vector can be normalized such that its largest element takes on a value of unity:

$$\{A^*\} = \frac{1}{\Lambda} \{A\} \tag{A-22}$$

where Λ is equal to the largest element of the design vector {A}. The element stiffness matrix and displacement vectors can be normalized similarly as

$$[K_i^*] = \frac{1}{\Lambda} [K_i] \tag{A-23}$$

and

$$\{r_i^*\} = \Lambda\{r_i\} \tag{A-24}$$

Thus

$$\frac{U_i}{U_i^*} = \frac{\frac{1}{2} \{r_i\}^t [K_i] \{r_i\}}{\frac{1}{2} \{r_i^*\}^t [K_i^*] \{r_i^*\}} = \frac{1}{\Lambda} \tag{A-25}$$

which may be written as

$$U_i = \frac{U_1^*}{\Lambda} \tag{A-26}$$

The expressions for the volume of the i^{th} element are

$$V_i = \rho A_i \ell_i \tag{A-27}$$

and

$$V_i^* = \rho A_i^* \ell_i \tag{A-28}$$

so

$$\frac{V_i}{V_i^*} = \frac{A_i}{A_i^*} = \Lambda \tag{A-29}$$

The optimality criterion derived requires that the strain energy density of each element attain an average or constant value as follows:

$$\frac{U_i}{V_i} = \delta = \frac{U_i}{V_i}_{avg} \tag{A-30}$$

which may also be expressed as

$$\frac{U_i^* / \Lambda}{V_i^* \Lambda} = \left(\frac{U_i}{V_i}\right) \tag{A-31}$$

or

$$\Lambda^2 = \frac{\eta^*_i}{(\eta_i)_{avg}} \tag{A-32}$$

where $()^*_i$ and $()_{i)avg}$ are the element strain energy density and average strain energy density of the structure.

Multiplying both sides of the equation by A_i^2 and taking the square root

$$\Lambda A_i + D_i \sqrt{\frac{\eta_i^*}{(\eta_i)_{avg}}} \tag{A-33}$$

The recursion relation can now be written as

$$(\Lambda A_i)_{v+1} = (A_i)_v \sqrt{\frac{\eta_i^*}{(\eta_i)_{avg}}} \tag{A-34}$$

where v and v + 1 correspond to present and next cycles of design, respectively.